

Stony Brook University



OFFICIAL COPY

The official electronic file of this thesis or dissertation is maintained by the University Libraries on behalf of The Graduate School at Stony Brook University.

© All Rights Reserved by Author.

Force Feedback for Endowrist Instruments

A Thesis Presented

by

Fang Lin

to

The Graduate School

in Partial Fulfillment of the

Requirements

for the Degree of

Master of Science

in

Mechanical Engineering

Stony Brook University

May 2011

Stony Brook University

The Graduate School

Fang Lin

We, the thesis committee for the above candidate for the
Master of Science degree, hereby recommend
acceptance of this thesis.

Yu Zhou – Thesis Advisor
Assistant Professor, Department of Mechanical Engineering

Chad Korach – Chairperson of Defense
Assistant Professor, Department of Mechanical Engineering

Anurag Purwar – Member
Research Assistant Professor, Department of Mechanical Engineering

This thesis is accepted by the Graduate School

Lawrence Martin
Dean of the Graduate School

Abstract of the Thesis

Force Feedback for Endowrist Instruments

by

Fang Lin

Master of Science

in

Mechanical Engineering

Stony Brook University

2011

The purpose of the project is to analyze current sensor designs, improve the design and fabricate a sensor attachment for the Endowrist Instruments. The predicament with the Endowrist Instruments is the lack of feedback regarding the interacting force between the gripper and the tissue. It is not safe to perform the surgery with Endowrist Instruments that do not give feedback, therefore only those surgeons with a great deal of experience can perform the surgery. Feedback can be added by attaching a sensor attachment to the instrument and the robot, but the problem is current sensor designs do not provide precise measurements. It will not be beneficial if there are any major changes to the infrastructure of the Endowrist Instruments, so the sensor attachment should be easily fit to the instrument and the robot. It will be located directly outside the input interface panel. To improve the design, all forces acting on the instrument must take into consideration. Some forces are difficult to measure, but this problem can be solved by applying some techniques. It is difficult to measure the supporting forces between the trocar and the instrument shaft; by using overcoat technique, the supporting forces can be measured. To measure the contact force between the instrument and the adapter, there must be two plates

between the instrument and the adapter; one plate should be fixed to the instrument and the other plate should be fixed to the adapter. When place sensors between these two plates, contacting forces between these two plates can be measured. A force analysis is required to fully understand the situation. After performing a force analysis, the theoretical relationship between the force in the tip of the gripper and the input torque can be found. However, calibration using LabVIEW will be able to find the true approximate relation.

Table of Contents

List of Figures	vii
List of Tables	xi
Acknowledgments	xii
Chapter 1 Introduction	1
1.1 Motivation and Background	1
1.2 Objective and Methodology	2
1.3 Thesis Structure	3
Chapter 2 Literature Review	6
2.1 Strain Gage Sensor	6
2.2 Overcoat Sensor	7
2.2.1 Trocar Type Overcoat Sensor	7
2.2.2 Basic Type Overcoat Sensor	7
2.2.3 Latest Overcoat Sensor	8
Chapter 3 Force and Moment Analysis	9
3.1 Overcoat Force Analysis	9
3.2 Endowrist Instrument Force and Moment Analysis	10
Chapter 4 Conceptual Design	15
4.1 Design Concepts	15
4.2 Concept Evaluation	19
4.3 Final Concept	20
Chapter 5 Detail Design	23
5.1 Final Design	23

5.2 Components	28
Chapter 6 Prototype	57
6.1 Fabrication Results	57
6.2 Circuitry	60
6.2.1 Sensor Circuits	60
6.2.2 PCB Board Circuits	62
Chapter 7 Experimental Setup	64
7.1 Frame Adjustment	64
7.2 Signal Processing	69
7.3 Calibration Equations	69
7.4 LabVIEW Programming	70
Chapter 8 Results and Discussion	73
8.1 Results	73
8.2 Discussion	78
Chapter 9 Conclusion and Future Work	79
9.1 Conclusion	79
9.2 Future Work	80
References	81

List of Figures

Figure 3.1 Overcoat Sensor Locations	9
Figure 3.2 Forces on Overcoat Tube	9
Figure 3.3 Forces and Moments on Endowrist Instrument	10
Figure 4.1 First Overcoat Sensor Assembly	15
Figure 4.2 Parallel-Plate Sensor Assembly	16
Figure 4.3 Torque Sensor	17
Figure 4.4 Second Overcoat Sensor Assembly	18
Figure 4.5 Latest Overcoat Assembly	19
Figure 5.1 Solid Model of Sensor Attachment	23
Figure 5.2 Torque Sensor Assembly	24
Figure 5.3 Bottom Plate Assembly	25
Figure 5.4 Top Plate Assembly	26
Figure 5.5 Sensor Attachment Assembly	27
Figure 5.6 Aluminum Tube	28
Figure 5.7 Overcoat Shaft Collar	29
Figure 5.8 C-Shape Wire Clip	30

Figure 5.9 Shaft Collar Block	31
Figure 5.10 Shaft Collar Plate	32
Figure 5.11 Thrust Bearing Plate	33
Figure 5.12 Overcoat Block	34
Figure 5.13 Locking Mechanism Plate	35
Figure 5.14 Locking Mechanism	36
Figure 5.15 Front Block	37
Figure 5.16 Middle Plate	38
Figure 5.17 Side Block	39
Figure 5.18 Rear Block	40
Figure 5.19 Rear Middle Block	41
Figure 5.20 Rear Sensor Block	42
Figure 5.21 Front Sensor Block	43
Figure 5.22 Front Left Plate	44
Figure 5.23 Front Right Plate	45
Figure 5.24 Front Block	46
Figure 5.25 Back Block	47

Figure 5.26 Front Strain Gage Sensor Block	48
Figure 5.27 Rear Strain Gage Sensor Block	49
Figure 5.28 Bottom Cover Plate	50
Figure 5.29 Top Wheel	51
Figure 5.30 Bottom Wheel	52
Figure 5.31 Support Fixture	53
Figure 5.32 Cantilever Beam	54
Figure 5.33 Left Rear Side Block	55
Figure 5.34 Right Rear Side Block	56
Figure 6.1 Locking Mechanism Plate	57
Figure 6.2 Torque Sensor Prototype	58
Figure 6.3 Bottom Plate Installed to the Robot Adapter	58
Figure 6.4 Instrument Shaft Inserted to Overcoat Tube	59
Figure 6.5 Middle Plate Assembly	59
Figure 6.6 Sensor Attachment with Endowrist Instrument	60
Figure 6.7 Sensor Circuit Diagram	61
Figure 6.8 PCB Board A	63

Figure 6.9 PCB Board B	63
Figure 7.1 Aluminum Frame	64
Figure 7.2 Adjust Frame Length	65
Figure 7.3 Plastic Strips Inserted to Sensor Attachment	66
Figure 7.4 Sensor Attachment Installed to Aluminum Frame	66
Figure 7.5 Calibrate Tip Force in X-Axis	67
Figure 7.6 Calibrate Tip Force in Y-Axis	68
Figure 7.7 Calibrate Tip Force in Z-Axis	68
Figure 7.8 Signal Processing Diagram	69
Figure 7.9 LabVIEW Front Panel	71
Figure 7.10 LabVIEW Block Diagram	72

List of Tables

Table 4.1 Concepts Evaluation	21
Table 4.2 Concept Comparison	22
Table 8.1 X-Axis Force Measurements	74
Table 8.2 Y-Axis Force Measurements	75
Table 8.3 Moment about X-Axis	76
Table 8.4 Z-Axis Force Measurement	77

Acknowledgments

I thank my advisor Professor Yu Zhou for his guidance and support during the past two years. I have gained extensive knowledge and research experience working under him.

I thank Kevin Ooh for helping me search for research papers.

I thank Xiao Chen for working on the calibration with me.

Special thanks to Mr. George and Mr. Lester from Stony Brook University machine shop for lending me tools to work in machine shop, and helping me machine complex parts.

Chapter 1 Introduction

1.1 Motivation and Background

A Da Vinci Surgical System is a robotic platform which is designed for surgeons to perform surgery. It has four components, Surgeon Console, Patient-side Cart, Endowrist Instrument and Vision System. The surgeon positions the patient to the Patient-side Cart, and he or she sits comfortably at the console to control the robot to perform the surgery. There are many types of Endowrist Instruments, and different instrument is to implement different task. The Vision System provides the vision feedback while the surgeon is performing the surgery.

Advantages of utilizing Da Vinci Surgical System to perform surgery include incision minimization, reduced blood loss, lesser pain and quicker recovery. With this technology, major surgeries can be implemented and some patients do not need hospitalization after the surgery. However, the robot does not provide force feedback. Surgeons sometimes break the string while suturing, and they have to clamp the tissue carefully during the surgery. If the instrument tip pressure exceeds 20 psi, then the tissue will be damaged. Therefore, only those surgeons with extensive experience are allowed to utilize Da Vinci Surgical System to perform surgery.

To add force feedback to the Da Vinci robot, a sensing unit is attached to the Endowrist Instrument to measure the force at the tip of the instrument. The Endowrist Instrument is used to imitate human hand movements, and it is a four degree of freedom mechanism. Even though there are different types of instruments, the mechanical design is same except the tip. All instruments have four pulley mechanisms, and the motion of the gripper is controlled by four wheels.

Existing sensor designs were done to measure the force at the tip of the instrument. There are two type sensor designs, strain gage sensor and overcoat sensor; there are three overcoat sensor designs. These sensor designs cannot provide accurate force measurement due to inadequacy of the design, so the new sensor design should eliminate these issues and satisfy the design requirement.

1.2 Objective and Methodology

To improve the accuracy of the sensor design, inadequate in the design should be reviewed. The new sensor design should satisfy requirements including, no major change to the infrastructure of the Endowrist Instrument, easy for installation, provide accurate force measurements, input torque measurement and the overcoat tube should be as small as possible to avoid changing trocar design.

The trocar and tissue contact forces with the instrument shaft are difficult to measure, therefore an overcoat technique should be applied to simplify the problem. The overcoat tube has to be long enough to cover the whole shaft, and the sensor should be located inside the tube to measure the contact force between the inner surface of the tube and the shaft.

The contact force between the instrument and the robot adapter can be measured utilizing Parallel-plates technique. A top plate is attached to the instrument, and the bottom plate is attached to the robot adapter; sensors are placed between these two plates to measure the contact force. It is easier to measure the force between two flat surfaces than two unusual surfaces. The robotic arm has four wheels that can apply torque to the instrument to control the motion, and the input torque can be measured utilizing the torque sensor. The torque sensor should be able to

rotate when engaged with the instrument wheels and not to constraint the instrument tip movement.

1.3 Thesis Structure

Chapter 2 reviews existing sensors which were developed by other people to measure the force at the tip of the instrument. There are two type sensor designs, strain gage sensor and the overcoat sensor. Strain gages are stuck to the instrument shaft to measure the two dimensional forces at the tip of the instrument is called strain gage sensor. A sensing unit that has an overcoat tube covers the instrument shaft and measure the three dimensional tip forces is called overcoat sensor. Pros and cons of each sensor will be discussed in this chapter.

Chapter 3 presents theoretical equations of the overcoat tube and the Endowrist Instrument. Tissue and trocar contact forces on the instrument shaft are difficult to measure, however this problem can be simplified utilizing overcoat technique. Contact force between the instrument adapter and the robotic arm adapter is difficult to measure, and the force can be measured utilizing parallel-plate technique. Input torque can be measured utilizing torque sensors. Assume it is static, force and moment equations can be derived.

Chapter 4 presents design concepts of the sensor attachment. The sensor attachment is designed to fit the Endowrist Instrument and the robotic arm adapter. The first concept is sensor attachment that does not have wire clips. The second concept is the special sensor attachment design. The third concept is the special overcoat design. Three concepts will be evaluated in this chapter, and the best concept would be the final concept.

Chapter 5 presents detail design of the sensor attachment. The sensor attachment is composed of an overcoat sensor, a parallel-plate sensor and the torque sensor. The overcoat

sensor assembly drawing from last chapter shows how the torque sensor is assembled together, and the parallel-plate sensor and torque sensor assembly drawings are shown in this chapter to illustrate how parts are assembled together. Detailed drawings show dimension of each component in the second section of the chapter, and it would be discussed in detail.

Chapter 6 presents the fabrication result and the circuit diagram. Locking mechanism plate, bottom plate, middle plate, torque sensor, overcoat tube and sensor attachment pictures are shown in this chapter. Overcoat sensor circuit, shaft collar block sensor circuit, parallel-plate sensor circuit and the torque sensor circuit are shown in the circuit diagram. Circuits are soldered to the PCB board, and the power supply provides power to circuits.

Chapter 7 presents experimental setup. The aluminum frame is clamped to the torque machine, and the sensor attachment is mounted to the frame. A string is hanging to the force machine and tied to the tip of the instrument, the applied force can be measured by the force gage while it is moving upward. Data can be obtained utilizing Signal Express and coefficients can be calculated by using Matlab, and then enter coefficients to LabVIEW to calibrate the sensor attachment.

Chapter 8 presents experimental result. The force gage measures the applied force, and the sensor attachment is calibrated to measure the tip force. Three trails data are recorded and the mean of measurements are calculated. Error can be determined by comparing applied force measured by force gage and the tip force measured by the sensor attachment.

Chapter 9 presents conclusion and the future work. The sensor attachment measures three-dimensional forces at the tip of the instrument and the moment about x-axis, and the design

can be improved to enhance the accuracy. Torque sensor and the overcoat tube should be redesigned, and the detail will be discussed in this chapter.

Chapter 2 Literature Review

Several papers were already published by various authors concerning this project. Some of the papers discussed the methodology, and others had sensor designs and experimental results. The papers that only discussed methodology will be referenced, while the other papers will be analyzed further in this chapter. There are two techniques that are used to measure the tip force: the strain gage sensor method and the overcoat sensor method.

2.1 Strain Gage Sensor

Bauernschmitt et al, stuck strain gages to the instrument shaft to measure the tip force. Sensors are located approximately one inch away from the forceps, and there are eight strain gages, “One full bridge for each direction in X and Y.” [1] The shaft bends when the force is applied to the tip, and as a result, strain gages change resistance.

The advantage of this method is that the forces perpendicular to the shaft can be measured. This method is relatively easy, and no design changes to the infrastructure of the instrument and the robot adapter are required. The trocar contact force can be ignored, and the strain gage sensor fits inside the trocar.

However, a disadvantage is that it cannot measure the forces parallel to the shaft. The tissue contact position can be at a half-inch away from the forceps, but the authors have ignored this force. As a result, the calibration will not be accurate. Since there are no sensors that measure the input torque, the compression force at both grippers cannot be measured. In addition, strain gages are exposed. When the instrument is inserted into the human body, there is contact between the sensor and the trocar. As a result, the strain gage coating will be scratched, and later it will peel off.

2.2 Overcoat Sensor

The overcoat sensor technique is different compared to the strain gage sensor. The overcoat sensor measures three-dimensional forces at the tip of the instrument, but the strain gage sensor only measures two-dimensional forces at the tip. Pros and cons of sensor designs will be analyzed in this chapter.

2.2.1 Trocar Type Overcoat

Shimachi et al. used overcoat type sensor to measure the force at the tip of the instrument. The sensing unit has two sensors: a trocar sensor and a hand side sensor [2]. This overcoat design measures three-dimensional forces at the tip of the instrument, and the trocar force is measured utilizing trocar sensor. The inner tube of the trocar sensor is made from stainless steel, and different instruments fit when insert to the tube.

The disadvantage of the trocar type sensor has two sensors, which is not convenient for installation. The gap between the inner tube of the trocar sensor and the instrument shaft introduces friction force that cannot be measured. In addition, the sensing unit does not have torque sensors to measure the input torque. As a result, the compression force at the tip of the instrument cannot be measured.

2.2.2 Basic Type Overcoat

Shimachi et al. utilized a basic overcoat tube method to measure three dimensional forces at the tip of instrument [3]. The overcoat tube has inner tube and outer tube, and it covers the instrument shaft. Tissue and trocar contact forces are acting on the outer tube instead of the shaft, and sensors are placed between inner and outer tubes to measure the contact force. Both

tubes are made from stainless steel, and the gap allows any Endowrist Instrument to fit to the overcoat tube.

Disadvantage of this method is the gap between the inner tube and the shaft introduces friction force which cannot be measured. The overcoat tube is connected to the sensor adapter through the universal joint, and the author ignored the supporting force. Additionally, this design does not have torque sensor to measure the input torque.

2.2.3 Latest Overcoat Sensor

The author utilized the latest overcoat sensor to measure three dimensional forces at the tip of the instrument. The overcoat tube has inner and outer tubes and it covers the instrument shaft; sensors are placed between tubes to measure the contact force, and the rubber seal prevents liquid pass through the space between the two tubes. Any Endowrist Instrument fits when install to the overcoat sensor, and it can be sterilized [4].

Disadvantage of the design is the gap between the inner tube and the instrument shaft introduces friction force. The tube is connecting to the sensor frame through the universal joint; however the author ignored the supporting force at the U-joint. The rubber seal between the inner and outer tubes introduce supporting force, and the force cannot be measured. The sensor frame is huge and heavy, so it does not fit to the robotic arm and the vibration is a problem. Additionally, the overcoat sensor does not have torque sensors to measure the input torque.

Chapter 3 Force and Moment Analysis

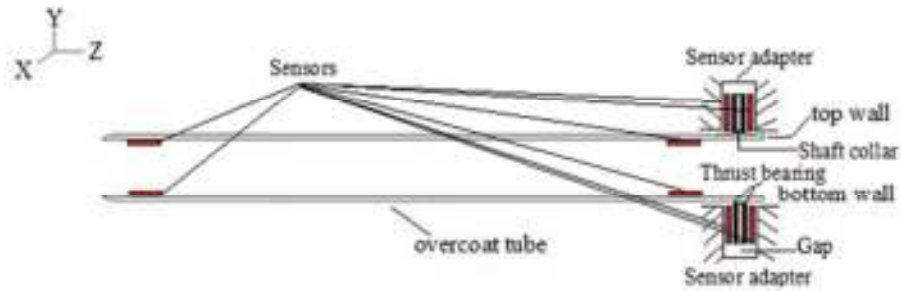


Figure 3.1 Overcoat Sensor Locations

The overcoat tube is connecting to the sensor adapter through the shaft collar. Pressure sensors are stuck to one side of thrust bearings, and the other side of bearings are contacting with the shaft collar to reduce the friction when rotating the tube. In the figure shown above, the gap eliminates the supporting forces at x-axis and y-axis.

3.1 Overcoat Tube Force Analysis

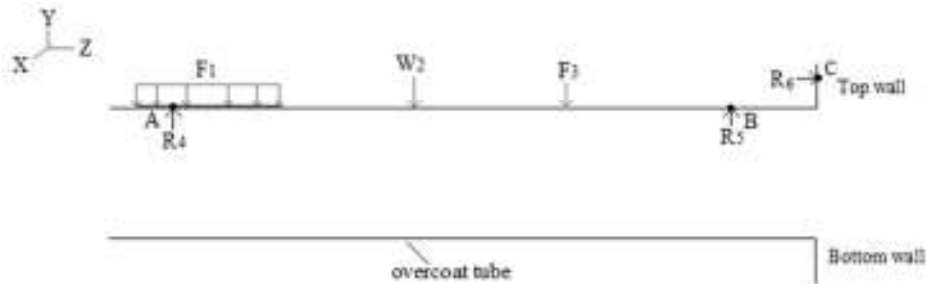


Figure 3.2 Forces on Overcoat Tube

F_1 : Tissue contact force

W_2 : Weight of the tube

F_3 : Trocar contact force

R₄: Supporting force at point A

R₅: Supporting force at point B

R₆: Supporting force at point C

Forces are acting on the overcoat tube instead of the instrument shaft when the shaft is inserted to the tube. Sensors are placed at points A, B and C to measure supporting forces. At point C, the supporting force in x-axis and y-axis equal to zero because of the gap. By assuming static, force equations can be derived.

Force equations are listed below:

$$\sum F_x = 0 = F_{1x} + W_{2x} + F_{3x} + R_{4x} + R_{5x} + R_{6x} \quad 3.1.1$$

$$\sum F_y = 0 = F_{1y} + W_{2y} + F_{3y} + R_{4y} + R_{5y} + R_{6y} \quad 3.1.2$$

$$\sum F_z = 0 = F_{1z} + W_{2z} + F_{3z} + R_{4z} + R_{5z} + R_{6z} \quad 3.1.3$$

3.2 Endowrist Instrument Force and Moment Analysis

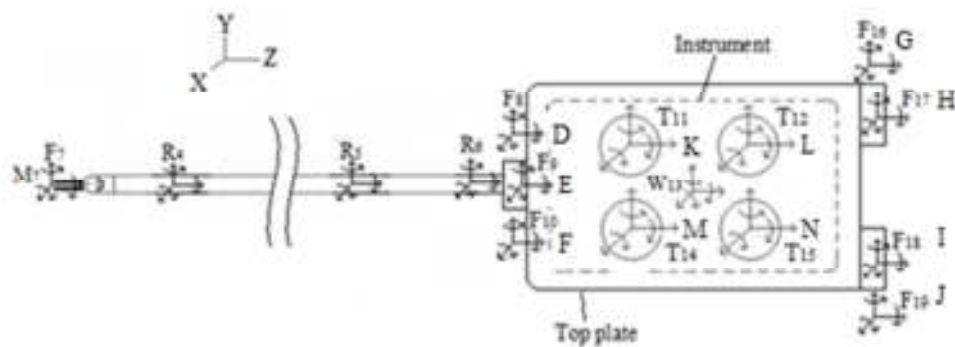


Figure 3.3 Forces and Moments on Endowrist Instrument

The top plate is attached to the instrument, and the force and moment equations can be derived by assuming static. Supporting forces on the instrument shaft are same as supporting forces in Figure 3.2.

F_7 : Force at the tip

F_8 : Contact force at point D

F_9 : Contact force at point E

F_{10} : Contact force at point F

W_{13} : Weight of the instrument and the top plate

F_{16} : Contact force at point G

F_{17} : Contact force at point H

F_{18} : Contact force at point I

F_{19} : Contact force at point J

M_7 : Moment at the tip

T_{11} : Torque on wheel K

T_{12} : Torque on wheel L

T_{14} : Torque on wheel M

T_{15} : Torque on wheel N

Force in x-axis, equation is listed below:

$$\sum F_x = 0 = F_{7x} + R_{4x} + R_{5x} + R_{6x} + F_{8x} + F_{9x} + F_{10x} + W_{13x} + F_{16x} + F_{17x} + F_{18x} + F_{19x}$$

$$R_{6x} = F_{8x} = F_{10x} = F_{16x} = F_{19x} = 0$$

$$F_{7x} = -R_{4x} - R_{5x} - F_{9x} - W_{13x} - F_{17x} - F_{18x} \quad 3.2.1$$

$$R_{6z} = R_{61z} + R_{62z} + R_{63z}$$

Moment about x-axis, equation is listed below:

$$\begin{aligned} \sum M_x = 0 = & M_{7x} + R_{4y} \cdot r_{4y} + R_{4z} \cdot r_{4z} + R_{5y} \cdot r_{5y} + R_{5z} \cdot r_{5z} + R_{61y} \cdot r_{61y} + R_{61z} \cdot r_{61z} + R_{62z} \\ & \cdot r_{62z} + R_{63z} \cdot r_{63z} + F_{8y} \cdot r_{8y} + F_{8z} \cdot r_{8z} + F_{9y} \cdot r_{9y} + F_{9z} \cdot r_{9z} + F_{10y} \cdot r_{10y} + F_{10z} \\ & \cdot r_{10z} + W_{13y} \cdot r_{13y} + W_{13z} \cdot r_{13z} + F_{16y} \cdot r_{16y} + F_{16z} \cdot r_{16z} + F_{17y} \cdot r_{17y} + F_{17z} \cdot r_{17z} \\ & + F_{18y} \cdot r_{18y} + F_{18z} \cdot r_{18z} + F_{19y} \cdot r_{19y} + F_{19z} \cdot r_{19z} + T_{11x} + T_{12x} + T_{14x} + T_{15x} \end{aligned}$$

$$\begin{aligned} M_{7x} = & -R_{4y} \cdot r_{4y} - R_{4z} \cdot r_{4z} - R_{5y} \cdot r_{5y} - R_{5z} \cdot r_{5z} - R_{61z} \cdot r_{61z} - R_{62z} \cdot r_{62z} - R_{63z} \cdot r_{63z} - F_{8y} \cdot \\ & r_{8y} - F_{9z} \cdot r_{9z} - F_{10y} \cdot r_{10y} - W_{13y} \cdot r_{13y} - W_{13z} \cdot r_{13z} - F_{16y} \cdot r_{16y} - F_{17z} \cdot r_{17z} - F_{18z} \cdot r_{18z} - F_{19y} \cdot \\ & r_{19y} - T_{11x} - T_{12x} - T_{14x} - T_{15x} \end{aligned} \quad 3.2.2$$

Force in y-axis, equation is listed below:

$$\sum F_y = 0 = F_{7y} + R_{4y} + R_{5y} + R_{6y} + F_{8y} + F_{9y} + F_{10y} + W_{13y} + F_{16y} + F_{17y} + F_{18y} + F_{19y}$$

$$R_{6y} = F_{9y} = F_{17y} = F_{18y} = 0$$

$$F_{7y} = -R_{4y} - R_{5y} - F_{8y} - F_{10y} - W_{13y} - F_{16y} - F_{19y} \quad 3.2.3$$

Moment about y-axis, equation is listed below:

$$\begin{aligned} \sum M_y = 0 = & M_{7y} + R_{4x} \cdot r_{4x} + R_{4z} \cdot r_{4z} + R_{5x} \cdot r_{5x} + R_{5z} \cdot r_{5z} + R_{6x} \cdot r_{6x} + R_{6z} \cdot r_{6z} + F_{8x} \cdot r_{8x} \\ & + F_{8z} \cdot r_{8z} + F_{9x} \cdot r_{9x} + F_{9z} \cdot r_{9z} + F_{10x} \cdot r_{10x} + F_{10z} \cdot r_{10z} + W_{13x} \cdot r_{13x} + W_{13z} \cdot r_{13z} \\ & + F_{16x} \cdot r_{16x} + F_{16z} \cdot r_{16z} + F_{17x} \cdot r_{17x} + F_{17z} \cdot r_{17z} + F_{18x} \cdot r_{18x} + F_{18z} \cdot r_{18z} + F_{19x} \\ & \cdot r_{19x} + F_{19z} \cdot r_{19z} + T_{11y} + T_{12y} + T_{14y} + T_{15y} \end{aligned}$$

$$T_{11y} = T_{12y} = T_{14y} = T_{15y} = 0$$

Input torques are in x axis only, so the input torque in y and z axis equal to zero.

$$\begin{aligned} M_{7y} = & -R_{4x} \cdot r_{4x} - R_{4z} \cdot r_{4z} - R_{5x} \cdot r_{5x} - R_{5z} \cdot r_{5z} - R_{6z} \cdot r_{6z} - F_{9x} \cdot r_{9x} - F_{9z} \cdot r_{9z} - W_{13x} \cdot r_{13x} - \\ & W_{13z} \cdot r_{13z} - F_{17x} \cdot r_{17x} - F_{17z} \cdot r_{17z} - F_{18x} \cdot r_{18x} - F_{18z} \cdot r_{18z} \end{aligned} \quad 3.2.4$$

Force in z-axis, equation is listed below:

$$\sum F_z = 0 = F_{7z} + R_{4z} + R_{5z} + R_{6z} + F_{8z} + F_{9z} + F_{10z} + W_{13z} + F_{16z} + F_{17z} + F_{18z} + F_{19z}$$

$$F_{8z} = F_{10z} = F_{16z} = F_{19z} = 0$$

$$F_{7z} = -R_{4z} - R_{5z} - R_{6z} - F_{9z} - W_{13z} - F_{17z} - F_{18z} \quad 3.2.5$$

Moment about z-axis, equation is listed below:

$$\begin{aligned} \sum M_z = 0 = & M_{7z} + R_{4x} \cdot r_{4x} + R_{4y} \cdot r_{4y} + R_{5x} \cdot r_{5x} + R_{5y} \cdot r_{5y} + R_{6x} \cdot r_{6x} + R_{6y} \cdot r_{6y} + F_{8x} \cdot r_{8x} \\ & + F_{8y} \cdot r_{8y} + F_{9x} \cdot r_{9x} + F_{9y} \cdot r_{9y} + F_{10x} \cdot r_{10x} + F_{10y} \cdot r_{10y} + W_{13x} \cdot r_{13x} + W_{13y} \cdot r_{13y} \\ & + F_{16x} \cdot r_{16x} + F_{16y} \cdot r_{16y} + F_{17x} \cdot r_{17x} + F_{17y} \cdot r_{17y} + F_{18x} \cdot r_{18x} + F_{18y} \cdot r_{18y} + F_{19x} \\ & \cdot r_{19x} + F_{19y} \cdot r_{19y} + T_{11z} + T_{12z} + T_{14z} + T_{15z} \end{aligned}$$

$$T_{11z} - T_{12z} - T_{14z} - T_{15z} = 0$$

$$\begin{aligned}
M_{7z} = & -R_{4x} \cdot r_{4x} - R_{4y} \cdot r_{4y} - R_{5x} \cdot r_{5x} - R_{5y} \cdot r_{5y} - F_{8y} \cdot r_{8y} - F_{9x} \cdot r_{9x} - F_{10y} \cdot r_{10y} - W_{13x} \cdot \\
& r_{13x} - W_{13y} \cdot r_{13y} - F_{16y} \cdot r_{16y} - F_{17x} \cdot r_{17x} - F_{18x} \cdot r_{18x} - F_{19y} \cdot r_{19y}
\end{aligned} \tag{3.2.6}$$

Chapter 4 Conceptual Design

Sensor attachment design concepts are based on theoretical equations. It should be able to measure: contact forces between the overcoat tube and the instrument shaft, contact force between the instrument adapter and the robotic adapter, and the input torque. The top plate has to fit to the instrument adapter, and the bottom plate should fit to the robotic arm adapter.

4.1 Design Concepts

Concept 1

The sensor attachment is composed of: an overcoat sensor, a parallel-plate sensor and four torque sensors. Overcoat sensor measures the supporting force between the overcoat tube and the instrument shaft. Parallel-plate sensor measures the contact force between the instrument adapter and the robotic arm adapter. Torque sensors measure the input torque, which is transferred from the robotic arm adapter wheels to instrument wheels.

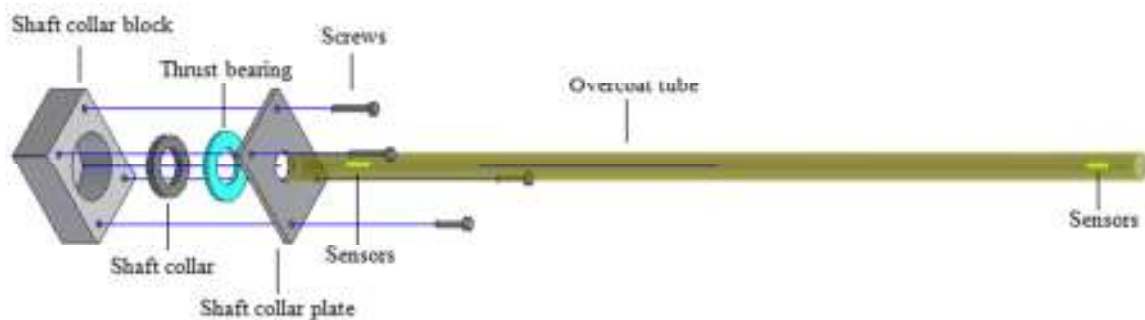


Figure 4.1 First Overcoat Sensor Assembly

The overcoat sensor consists of the following: an overcoat tube, a shaft collar, a shaft collar block, a shaft collar plate and sensors. Rubber is sheared to have same shape as the force sensing resistor sensing area and stick to sensors, and then glued to the inner surface of the tube.

There is no gap when insert the instrument shaft to the tube due to the flexibility of the rubber. The overcoat tube covers the instrument shaft and it is connecting to the sensor attachment adapter through the shaft collar. The shaft collar is press fitted to the tube and the shaft collar supporting forces perpendicular to the shaft equal to zero, the supporting force parallel to the shaft cannot be measured due to the inadequate of the design.

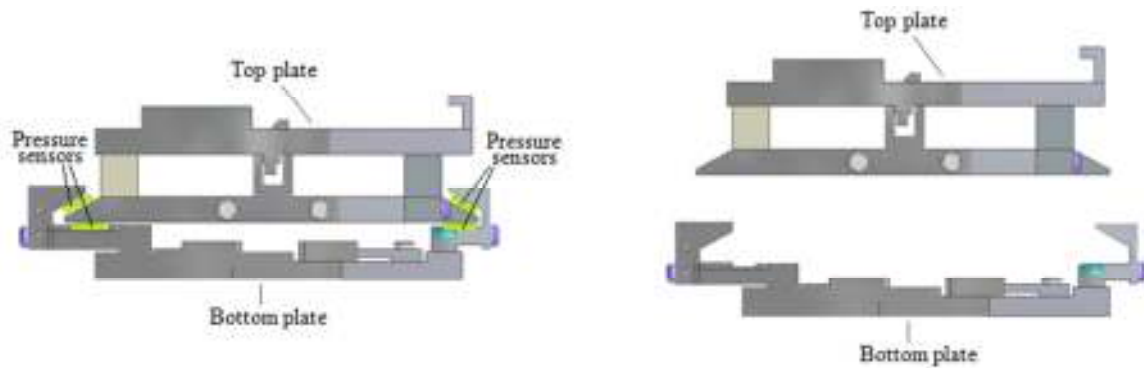


Figure 4.2 Parallel-Plate Sensor Assembly

Parallel-plate sensor assembly consists of a top plate, a bottom plate and pressure sensors. In Figure 4.2, the top plate is sitting on the top of the bottom plate. Pressure sensors are stuck to contact points between these two plates to measure contact force. Figure at the right-hand side shows how the top plate and bottom plate look like.

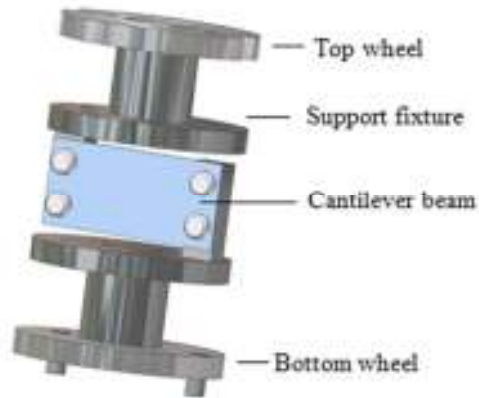


Figure 4.3 Torque Sensor

The torque sensor consists of the following: a top wheel, a bottom wheel, two support fixtures, a cantilever beam and the full-bridge strain gage. The strain gage is mounted to the cantilever beam to measure the input torque. If the top wheel is fixed, the cantilever beam bends by rotating the bottom wheel.

An advantage of this design is that it measures three-dimensional forces at the tip of the instrument. Sensors are glued to the inner surface of the tube and the rubber is placed on the sensor. As a result of this, there is no gap when inserting the instrument shaft to the tube, due to the flexibility of the rubber. The torque sensor measures the input torque. In addition, changing the infrastructure of the Endowrist Instrument is not required of this design. However, there are no wire clips to hold the wires inside of the overcoat tube, and as such the sensors can be damaged easily.

Concept 2

The sensor attachment consists of the following: an overcoat sensor with wire clips, a parallel plate sensor and four torque sensors. The difference between this design and the

previous one are the overcoat sensor design and the parallel plate sensor design. Torque sensor design is same as the one in the first concept.

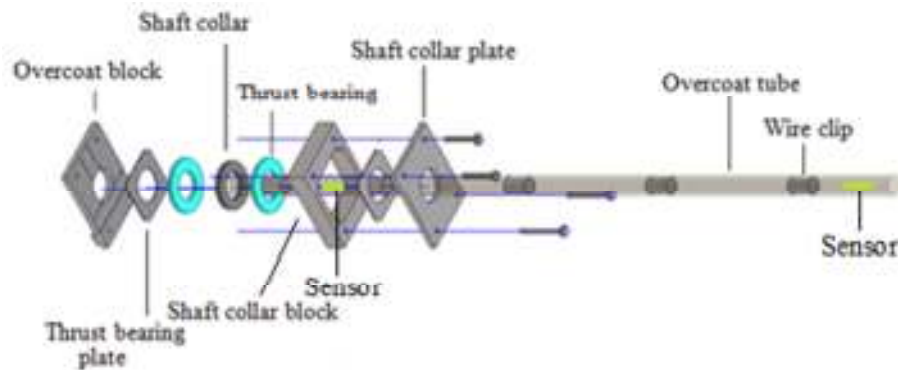


Figure 4.4 Second Overcoat Sensor Assembly

The overcoat consists of the following: an overcoat block, two thrust bearing plates, two thrust bearings, a shaft collar, a shaft collar block, a shaft collar plate, an overcoat tube and five wire clips. Shaft collar is press fitted to the overcoat tube; thrust bearings are required to reduce friction force while rotating the tube. Bearings are at the left-hand side and right-hand side of the shaft collar. To avoid damaging pressure sensors, there is no direct contact between sensors and the thrust bearings. Sensors are stick to one side of thrust bearing plates, and the other side of plates has contact with bearings. Wire clips are used to clamp wires inside the overcoat tube to avoid damaging sensors while insert instrument shaft into the tube.

Concept 3

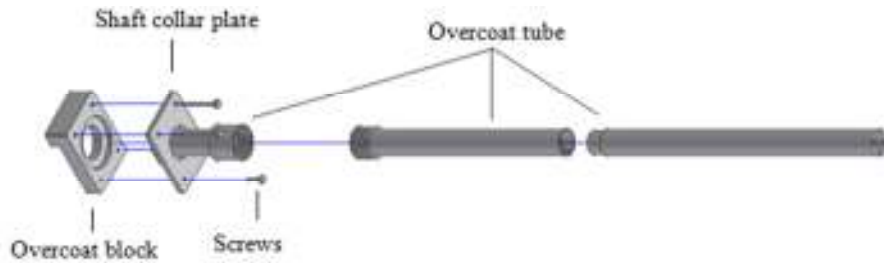


Figure 4.5 Latest Overcoat Assembly

The only difference between second concept and third concept is the overcoat design. The overcoat has three tubes, and sensors are stick to the inner surface of the longest tube and the shortest tube. One side of these two tubes have inner flat surface, and it is easier to stick sensors to flat surface than round surface. There are four long holes along the tubes to allow wires to passing through and avoid damaging sensors. The problem is this is a complex design, and it cannot be manufactured in the machine shop.

4.2 Concept Evaluation

In the first concept, the overcoat tube does not have wire clips, so sensors can be damaged easily when insert the instrument shaft into the tube. Top plate is sitting on the top of pressure sensors and sensors above are positioned at an angle to measure two-dimensional forces at that location; it would be better to use two sensors to measure two dimensional forces separately at that point instead of one.

In the second concept, five wires clips are installed to the overcoat tube to hold wire and avoid damaging sensors while inserting instrument shaft to the tube; it is difficult to put in wire clips to the tube. Pressure sensors are positioned horizontally or vertically at each contact point between the top plate and bottom plate to measure contact force.

In the third concept, the overcoat design is different compared to first two concepts. Sensors are stick to the inner surface of the longest tube and the shortest tube. Sensor wires are passing through four holes along the overcoat tube, so no wire clips necessary. The overcoat design cannot be machined due to complex shape and design.

4.3 Final Concept

Criteria I

A: Originality – The design must not be patented, and it must contain details no other design has.

B: Size – The design must fit to the robot arm adapter and Endowrist Instrument.

C: Precision – The design should be able to measure tip force with high precision.

D: Durability – The design should be able to handle vibration when installed to the robot.

E: Reliability – The design must be reliable.

F: Cost – The product must be cheap.




Concept			
Criteria	1	2	3
A	-	S	S
B	+	+	S
C	-	+	+
D	-	S	S
E	-	S	S
F	S	S	-
Σ^+	1	2	1
Σ^-	4	0	1
ΣS	1	4	4

Table 4.1 Concepts Evaluation

Criteria II

G: Lifetime – The design must have a long lift cycle.

H: Accuracy – The design must be able to provide results with an accuracy of ± 0.04 pound force.

I: Precision – The design must constitute enough data to extrapolate the average torque calculated.

J: Functionality – The design must perform its tasks without complications.

Objective	Weight Factor	Rating			Weight Factor x Rating		
		Concept 1	Concept 2	Concept 3	Concept 1	Concept 2	Concept 3
G	3	2	4	4	6	12	12
H	5	3	4	4	15	20	20
I	5	3	4	4	15	20	20
J	4	4	4	3	16	16	12
		Total			52	68	64

Table 4.2 Concepts Comparison

Based upon evaluation and comparison of different conceptual design, concept two has been chosen to be the final concept. It has the highest lifetime, accuracy, precision and functionality, as it is cost effective. First concept does not have wire clips inside the tube to hold wires, so sensors can be damaged easily. The overcoat tube is connecting to the sensor adapter through the shaft collar, and the supporting force cannot be measured. Second concept has wires clips to hold wires inside the tube to avoid damaging sensors, and the shaft collar supporting force can be measured. Third concept has complex overcoat design, and the tube cannot be manufactured in machine shop.

Chapter 5 Detail Design

The sensor attachment is composed of an overcoat sensor, a parallel plate sensor and four torque sensors. Figure 4.4 shows how the overcoat sensor is assembled together. Detailed drawings and assembly drawings are shown in this chapter; detailed drawing shows dimension of each part, and assembly drawing shows how parts are assembled together.

5.1 Final Design



Figure 5.1 Solid Model of Sensor Attachment

The top plate is designed to fit the Endowrist Instrument, and the locking mechanism in the plate is used to hold the instrument adapter in place; once the instrument adapter is inserted to the top plate, the locking mechanism will lock automatically and hold the adapter, and it is located at the center of the locking mechanism plate. Wire clips inside the tube hold wires to avoid damaging sensors while inserting instrument shaft to the tube. Torque sensors can rotate and move vertically; the torque sensor engage to instrument wheel, it transfers and measures the input torque at the same time. The bottom plate has a rectangular groove; the robotic arm

adapter wheels move up to engage with torque sensors, and the adapter holds the sensor attachment in place.

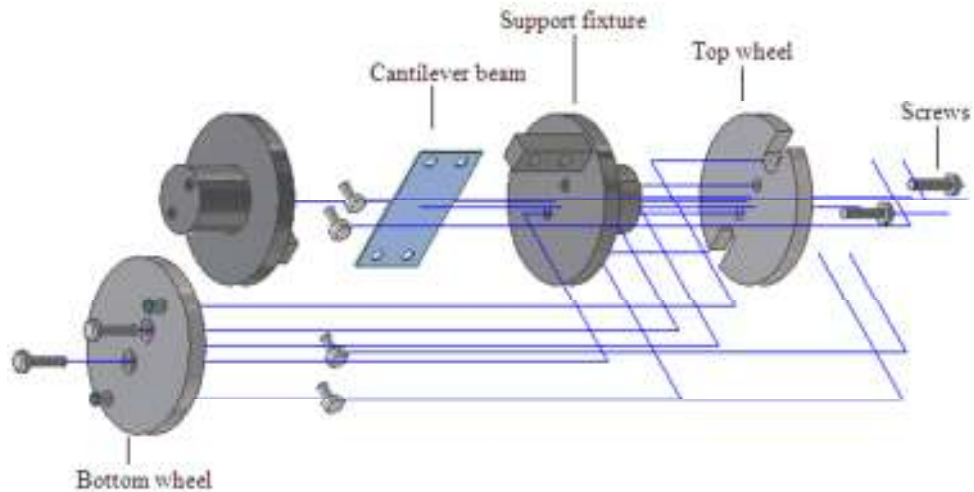


Figure 5.2 Torque Sensor Assembly

The figure shown above indicates how the torque sensor is assembled together. There are two support fixtures; one is fastened to the top wheel and the other one is screwed to the bottom wheel. The cantilever beam is screwed to both support fixtures, and the strain gage is stick to the center of the beam. The deflection of the cantilever beam depends on the thickness of the beam and the applied torque. When torque is applied, deflection decreases as the thickness of the beam increases.

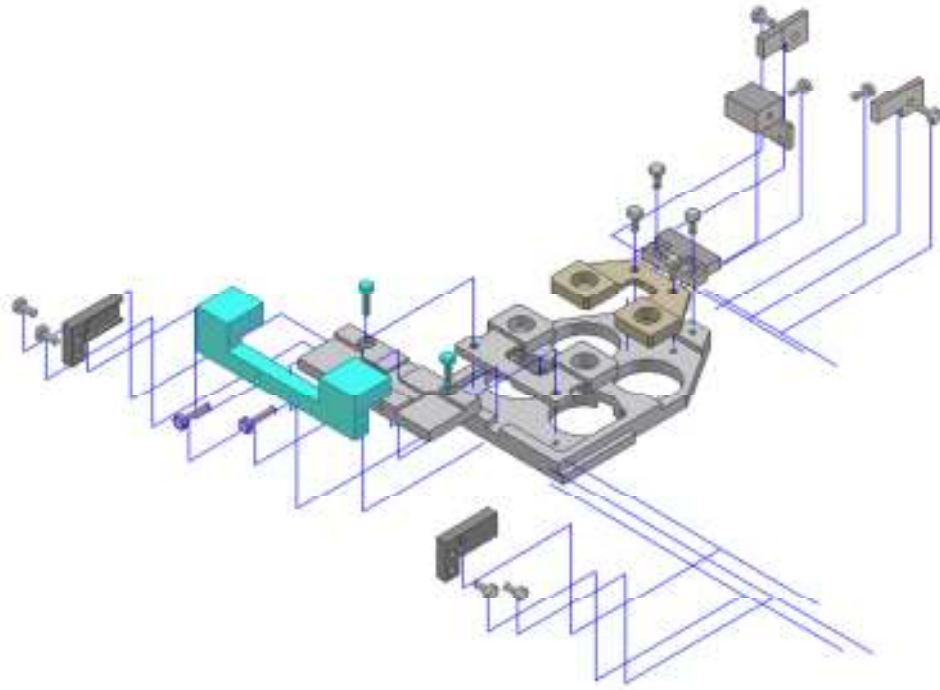


Figure 5.3 Bottom Plate Assembly

The figure shown above indicates how the bottom plate is assembled together. N-shape sensor blocks are screwed to the bottom cover plate, and torque sensors are installed into these two large holes to measure input torques. Other parts are fastened to the aluminum plate to clamp the top plate to the bottom plate, and pressure sensors are mounted to every contact point between the top plate and the bottom plate to measure the contact force.

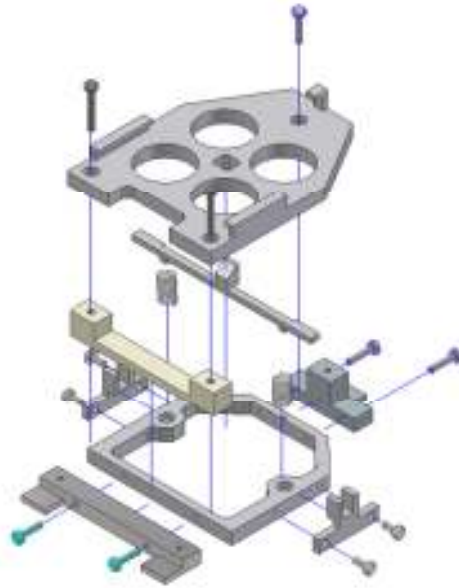


Figure 5.4 Top Plate Assembly

The figure shown above indicates how top plate is assembled together. The center of the top cover plate has a rectangle slot; the knob of the locking mechanism is passing through the slot. Springs are compressed by pressing the locking mechanism, and then the instrument can be removed from the sensor attachment. Other parts are assembled to the top cover plate, so the top plate can be clamped to the bottom plate.

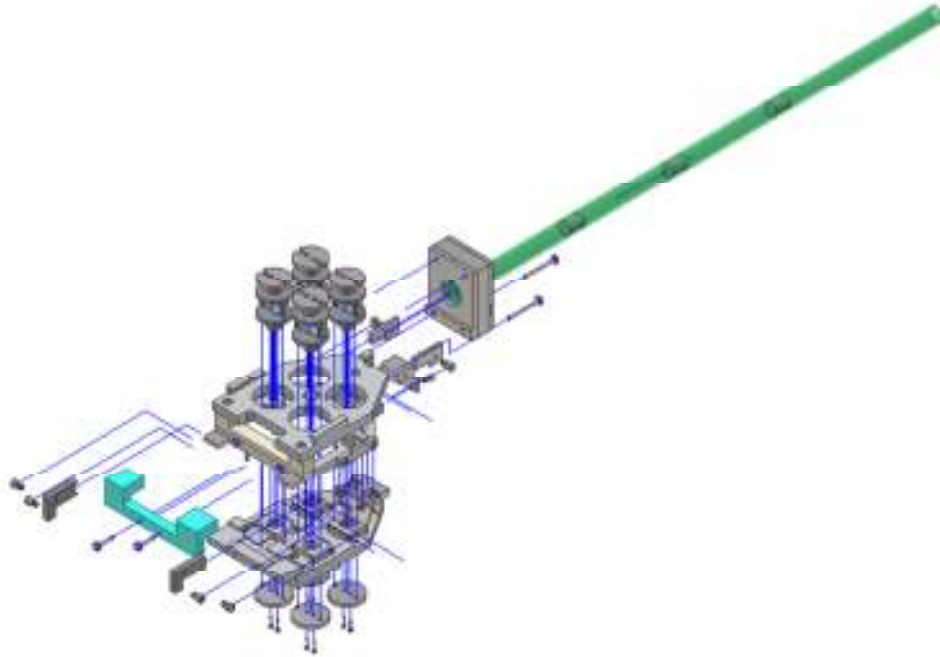


Figure 5.5 Sensor Attachment Assembly

The figure above shows how the sensor attachment is assembled together. Overcoat sensor is screwed to the top plate with two long screws, and the height of the tube is adjustable to allow the instrument shaft to insert to the tube when install the instrument to the top plate. The top plate is clamped to the bottom plate, and torque sensors are assembled to the bottom plate as well.

5.2 Components

Overcoat tube

Material: Aluminum (Alloy 6061)

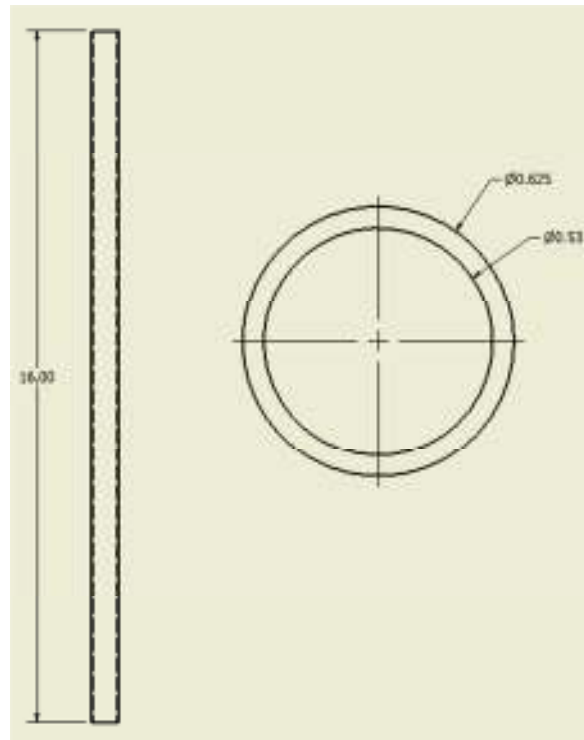


Figure 5.6 Aluminum Tube

The instrument shaft is about 16.5 inches long, so the overcoat tube should be at least 16 inches long to cover the shaft. The tube diameter should be as small as possible in order to insert into the trocar. Sensors are stick to the rubber and then glue to the inner surface of the tube, and the thickness is about 0.1 inch. The shaft diameter is about 0.33 inch, the inner diameter of the tube can be calculated by adding the thickness of sensors. The tube is a hollow cylinder and sensors are stick to the top, bottom, left and right. The inner diameter is 0.53 inch so the shaft can fit.

Shaft Collar

Material: Delrin

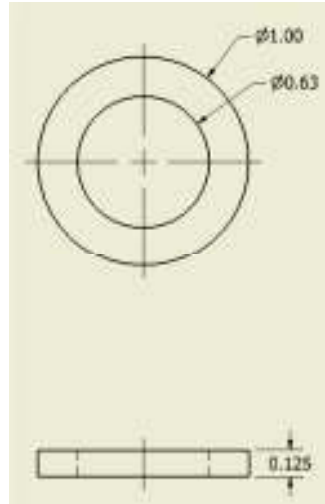


Figure 5.7 Overcoat Shaft Collar

The overcoat tube is purchased from McMaster, and the outer diameter is slightly larger than 0.625 inch because of the tolerance. The shaft collar inner diameter is slightly smaller than 0.63 inch and is press fitted to the tube. Two thrust bearings are used to reduce the friction while rotating the tube, and the shaft collar is placed between these two bearings. The thickness of the hollow cylinder is designed to be thin to reduce the shaft collar block thickness.

Wire Clip

Material: Aluminum 6061 Sheet Metal

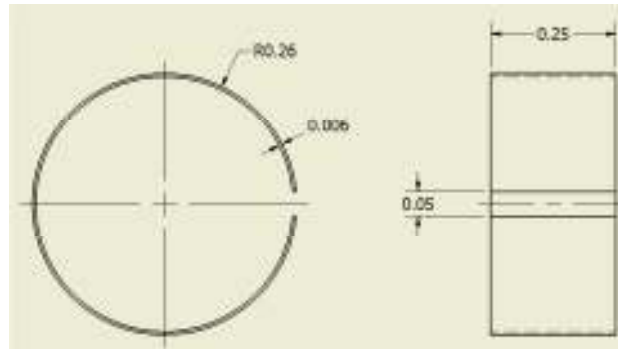


Figure 5.8 C-Shape Wire Clip

The wire clip is used to hold wires inside the overcoat tube to avoid damaging sensors while inserting instrument shaft to the tube. It is designed to be C-shape and it is very thin; it changes diameter by applying force to the top of the clip. As long as it is within the elastic region, the clip changes back to original shape when unloaded. The outer diameter is larger than the inner diameter of the tube, so the wire clip can be compressed and insert to the tube.

Shaft Collar Block

Material: Aluminum (Alloy 6061)

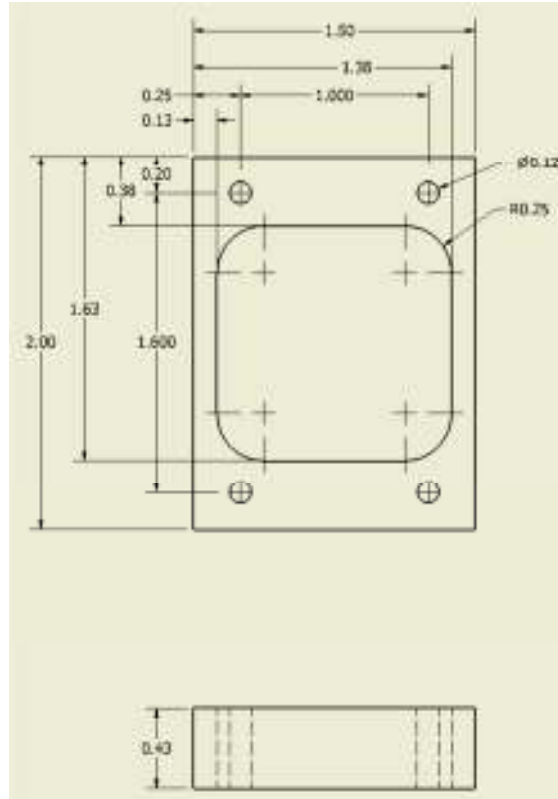


Figure 5.9 Shaft Collar Block

The shaft collar block has a large rectangle cutout at the center allows the shaft collar, thrust bearings and thrust bearing plates to fit in. The cutout is rectangle instead of circle is because the thrust bearing plate is square shape with chamfer corners.

Shaft Collar Plate

Material: Aluminum (Alloy 6061)

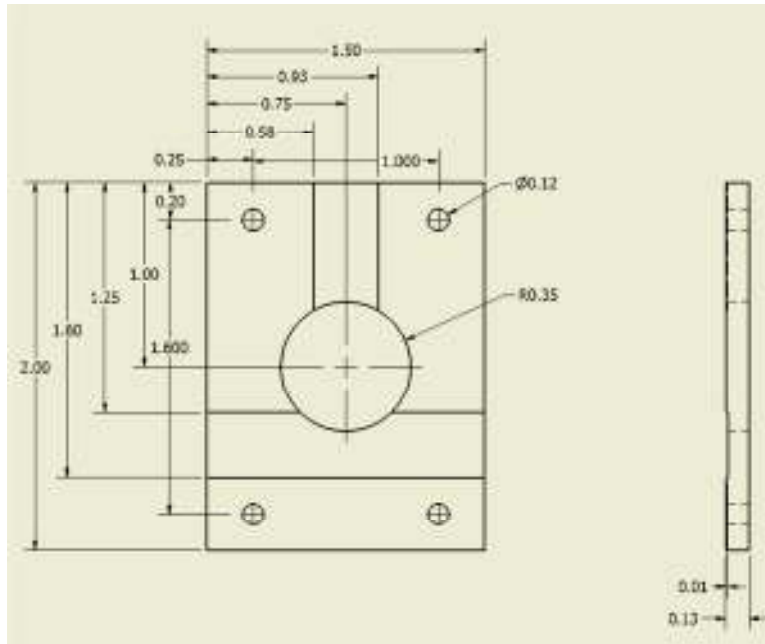


Figure 5.10 Shaft Collar Plate

The shaft collar plate has two rectangular slots, and it is 0.01 inch deep. Three pressure sensors are stick to these two slots; one sensor is placed in vertical, and others are in horizontal. Rubber is stick to sensors and then contacting with the thrust bearing plate. There is a large hole at the center of the plate allows the shaft to pass through.

Thrust Bearing Plate

Material: Aluminum (Alloy 6061)

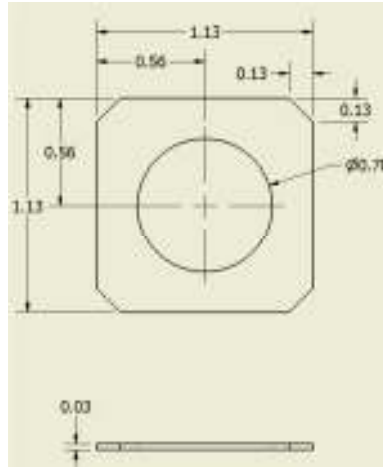


Figure 5.11 Thrust Bearing Plate

Shaft collar is placed between two thrust bearings to reduce friction while rotating the tube. Sensors are stick to one side of the thrust bearing plates, and the other side of plates are contacting with thrust bearings. Using thrust bearing plate instead of washer is because the plate has more space to stick pressure sensors than the washer.

Overcoat Block

Material: Aluminum (Alloy 6061)

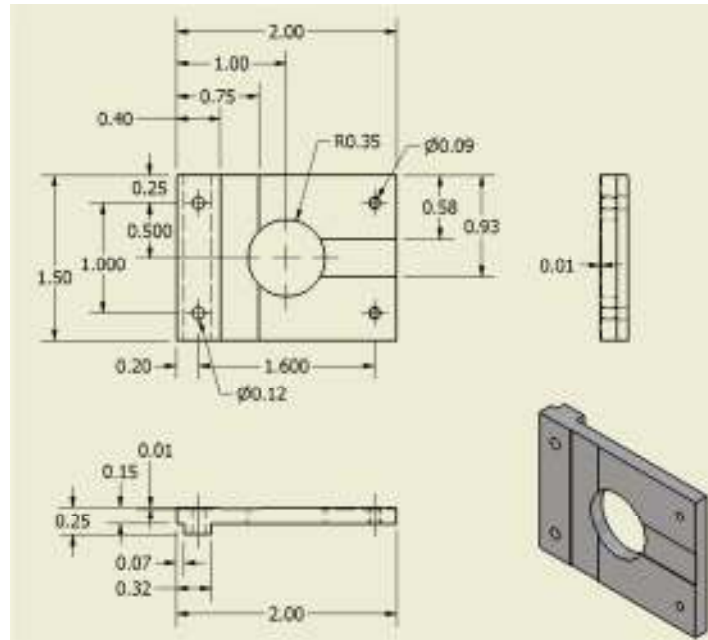


Figure 5.12 Overcoat Block

The overcoat block has two rectangular slots that is slightly larger than the pressure sensor sensing area diameter, and it is 0.01 inch deep. Pressure sensors are stick to these two slots, and the thrust bearing plate is stick to sensors. The large hole at the center of the block allows the overcoat tube to pass through.

Locking Mechanism Plate

Material: Material: Aluminum 6061

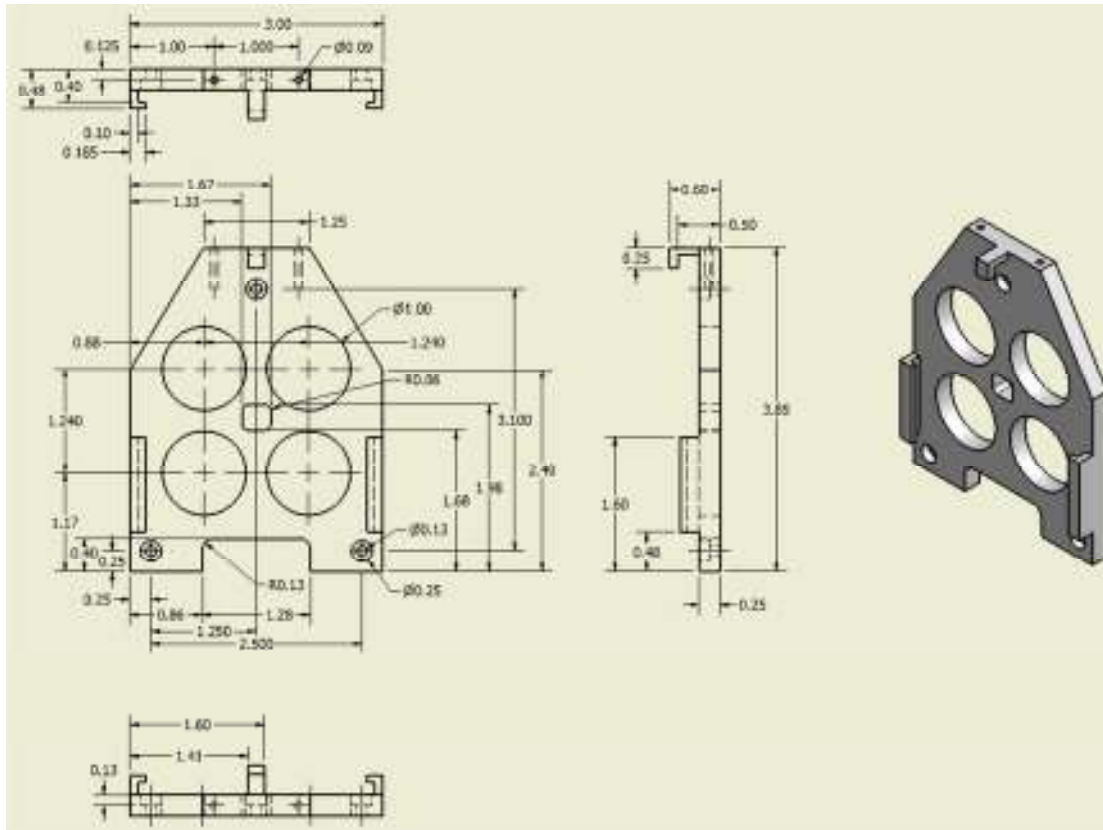


Figure 5.13 Locking Mechanism Plate

The locking mechanism plate is designed to fit the instrument adapter. The plate has four large holes to fit torque sensors. There is a rectangle slot at the center of the plate; the lock mechanism knob fits to the slot. Two tapped holes in the front of the plate allows the overcoat sensor to be assembled to the plate.

Locking Mechanism

Material: Aluminum 6061

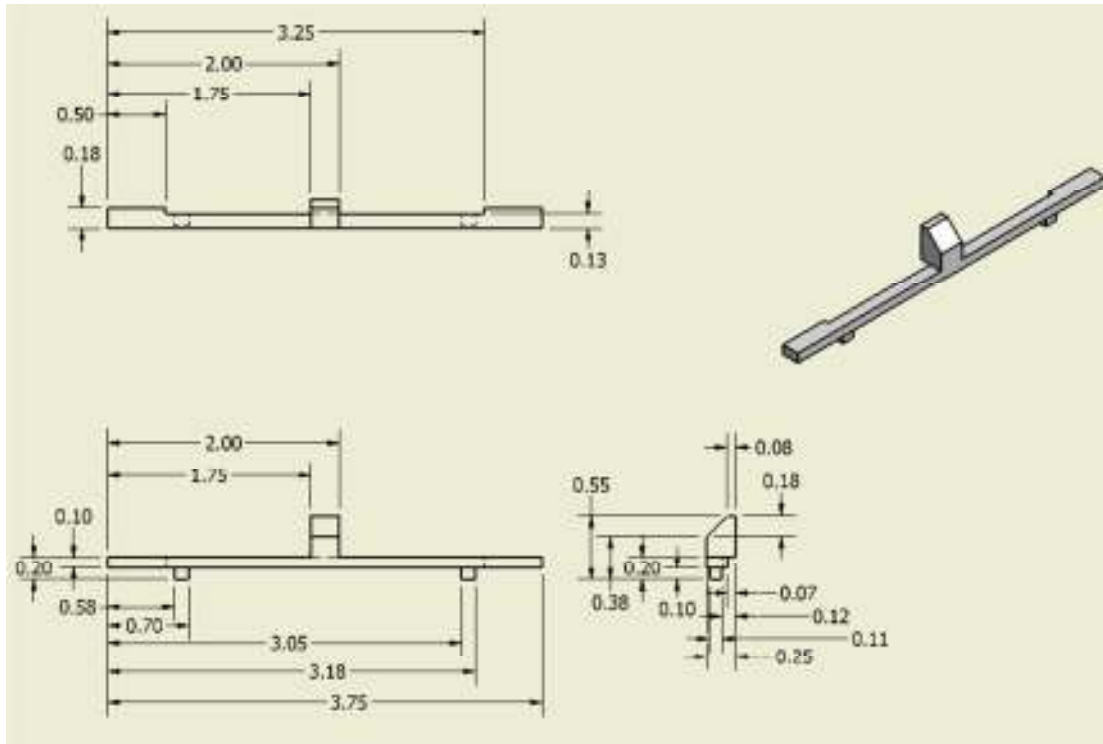


Figure 5.14 Locking Mechanism

The locking mechanism is made from aluminum bar, and the triangular shape knob fits to the rectangle slot of the locking mechanism plate. There are two square knobs underneath; springs will install to these knobs. The locking mechanism will lock automatically when insert the instrument adapter to the top plate; by pressing the locking mechanism, the instrument will be unlocked from the top plate and then take it out from the plate.

Front Block

Material: Aluminum 6061

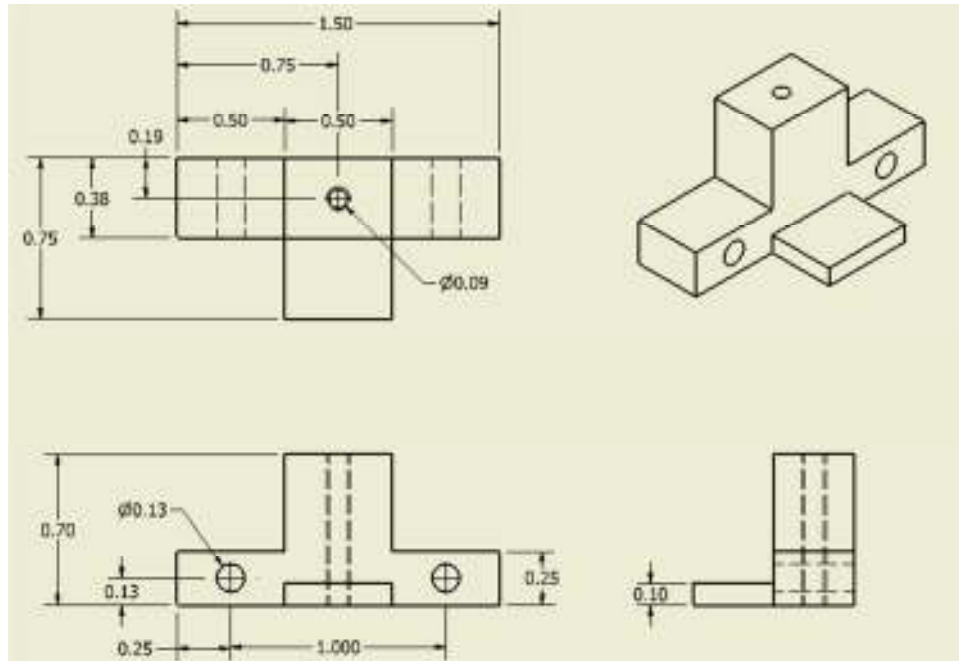


Figure 5.15 Front Block

The block has two clearance holes and one tapped hole. It is screwed to the middle plate through clearance holes, and the tapped hole allows it to fasten to the locking mechanism plate. The block is clamped to the bottom plate, and pressure sensors are placed between the block and the plate to measure the contact force.

Middle Plate

Material: Aluminum 6061

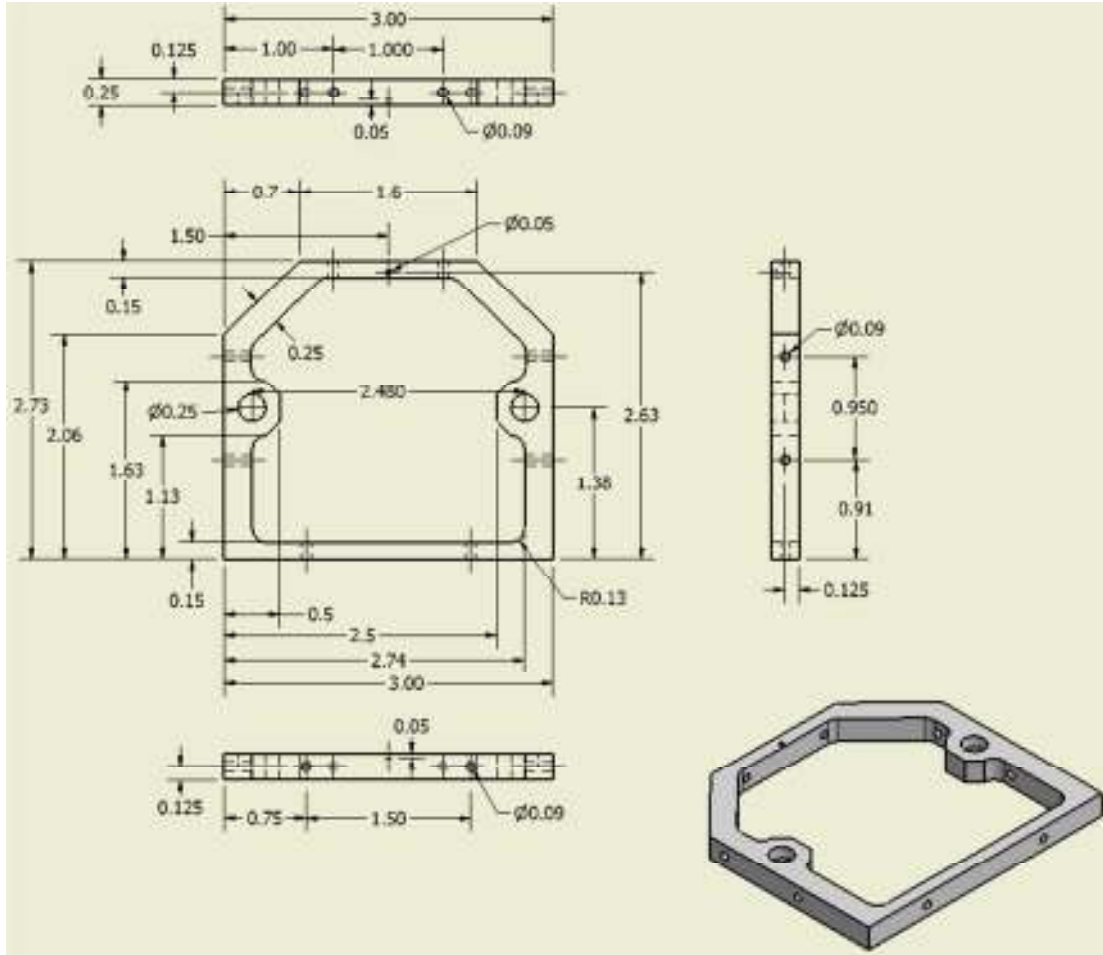


Figure 5.16 Middle Plate

The middle plate has a huge cutout at the center. There are two 0.25 inch diameter holes on the plate; two springs are install to the locking mechanism would be located in these holes. There are two tapped holes in the left-hand side and right-hand side of the plate; two side blocks will be screwed to these tapped holes. The front block is fastened to the front of the plate, and the rear middle block is screwed to the rear of the plate.

Side Block

Material: Aluminum 6061

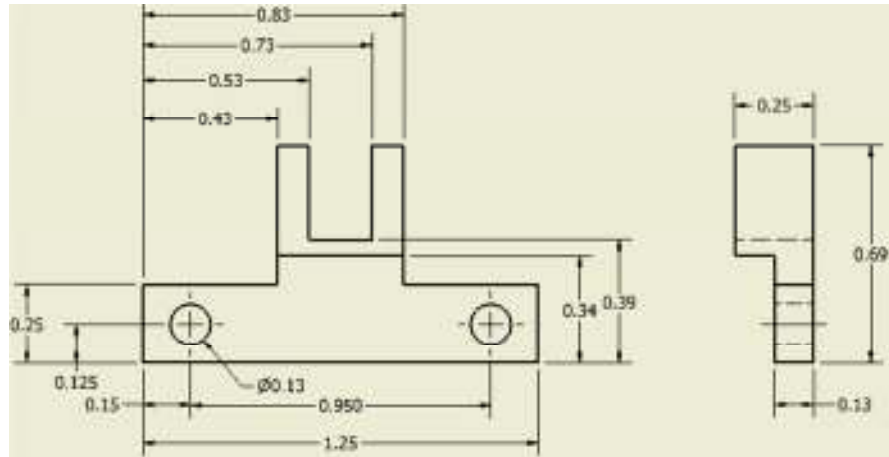


Figure 5.17 Side Block

The rectangle cutout, 0.2 inch by 0.3 inch at the middle of the block limits the locking mechanism movement in vertical direction only. From the front view of the block, two cutout, 0.43 inch by 0.44 inch at the left-hand side and right-hand side reduces weight of the block. The block is screwed to the middle plate through two 0.13 inch diameter clearance holes.

Rear Block

Material: Aluminum 6061

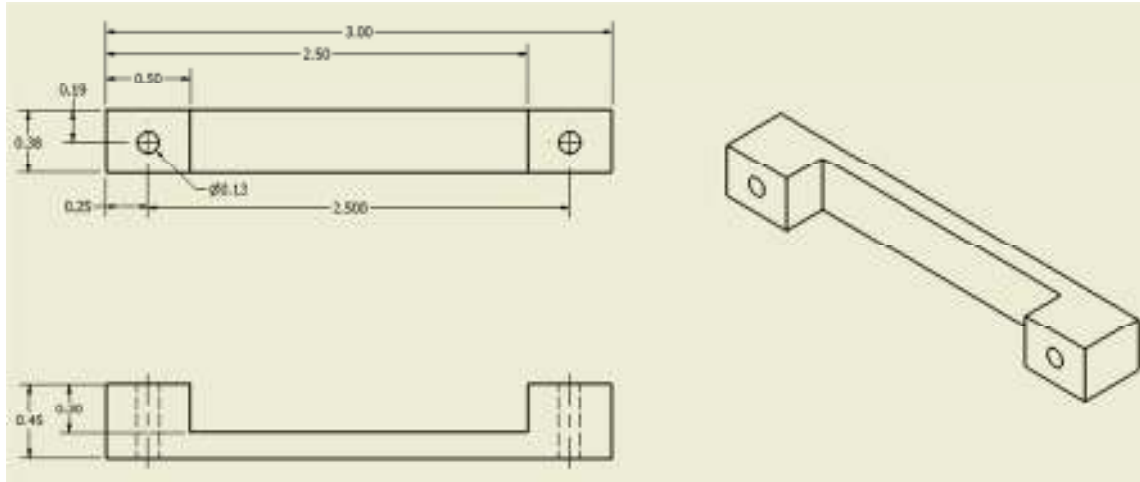


Figure 5.18 Rear Block

The rear block is made from aluminum bar. It is fastened to the locking mechanism plate and the rear middle block through two clearance holes. The rectangle cutout, 2 inch by 0.3 inch reduces the weight of the block.

Rear Middle Block

Material: Aluminum 6061

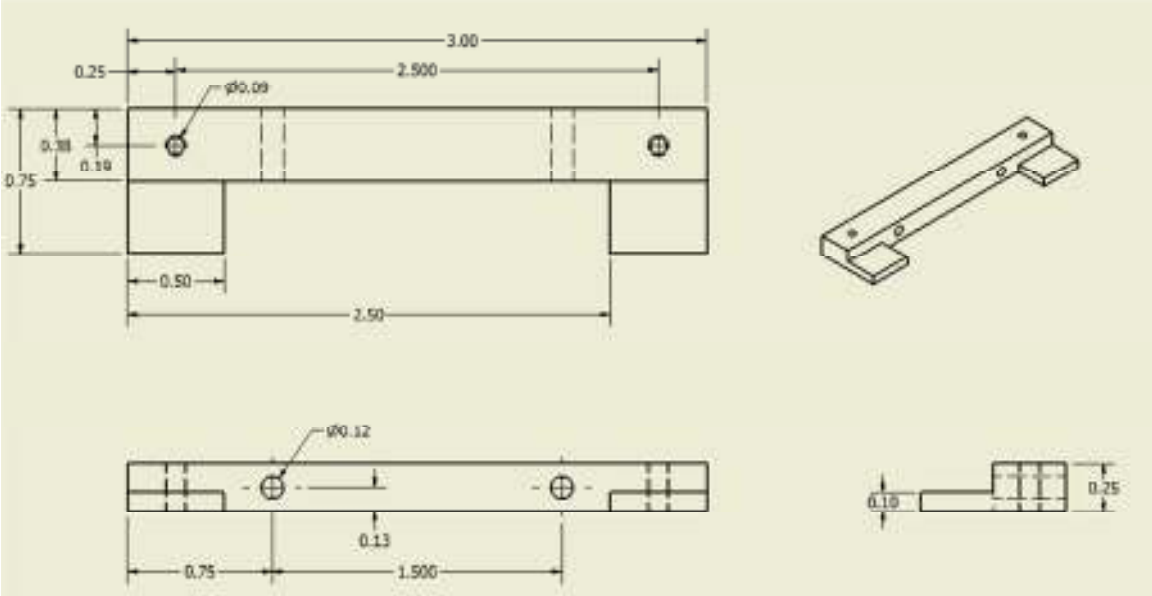


Figure 5.19 Rear Middle Block

The rear middle block has two clearance holes and two tapped holes. It is screwed to the middle plate through clearance holes, and it is fastened to the rear block and locking mechanism plate through tapped holes. The rectangle cutout, 2 inch by 0.37 inch reduces the weight of the block. This block is clamped to the bottom plate; pressure sensors are stick the contact points between the block and the bottom plate.

Rear Sensor Block

Material: Aluminum 6061 Sheet Metal

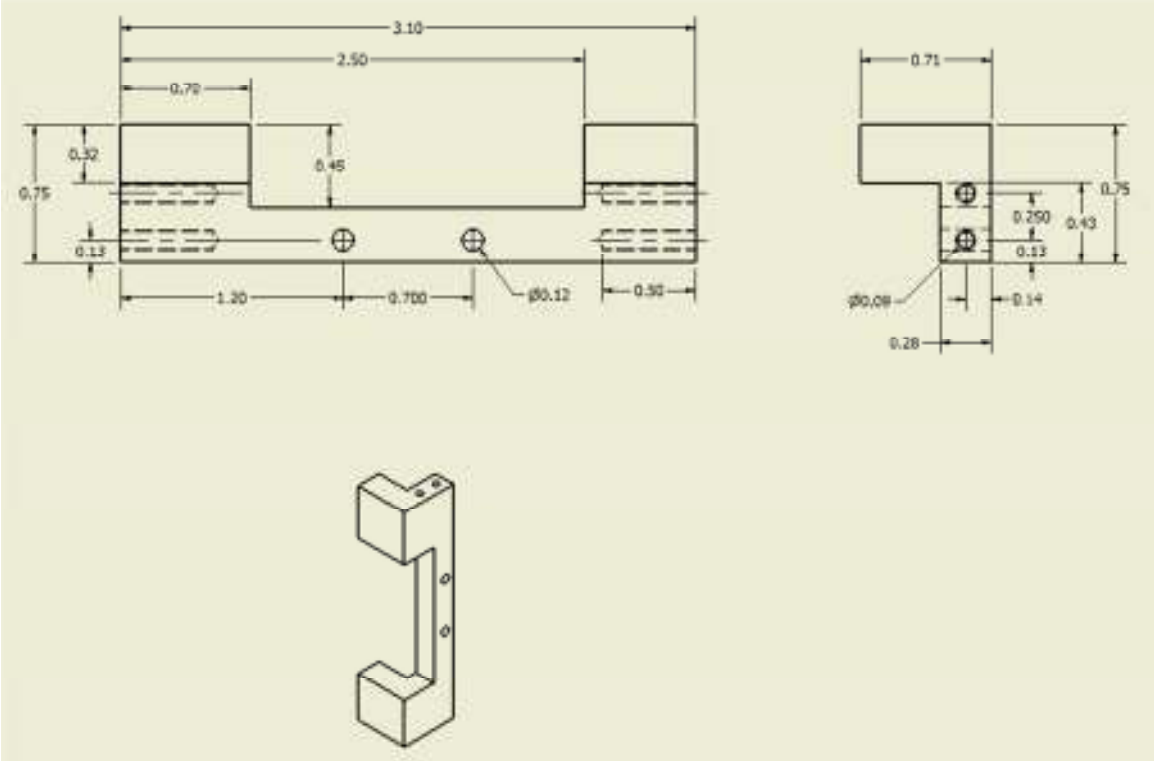


Figure 5.20 Rear Sensor Block

The rear sensor block is a part of the bottom plate. It has two clearance holes and four tapped holes. This block is screwed to the back block through clearance holes, and rear side blocks are fastened to both sides of the block. The rectangle cutout reduces the weight of the block, and sensors wires can come out from the cutout.

Front Sensor Block

Material: Aluminum 6061

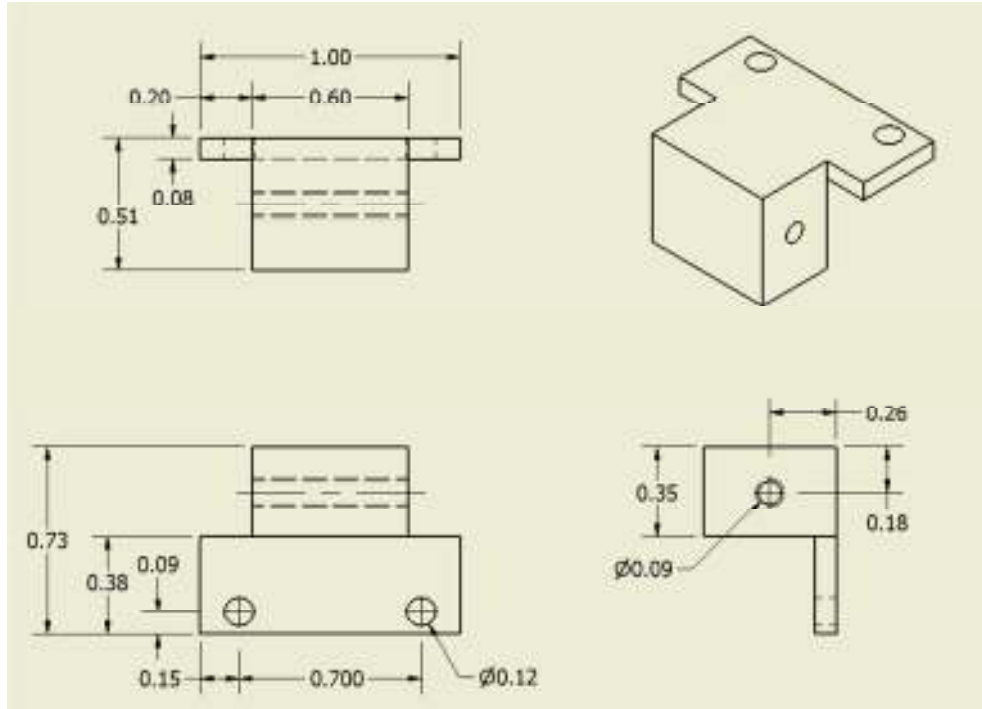


Figure 5.21 Front Sensor Block

The front sensor block has two clearance holes and a tapped hole. The block is screwed to the bottom cover plate through two clearance holes, and front plates are fastened to the tapped hole. Pressure sensors are placed at contact surfaces between the block and the top plate to measure the contact force.

Front Left Plate

Material: Aluminum 6061

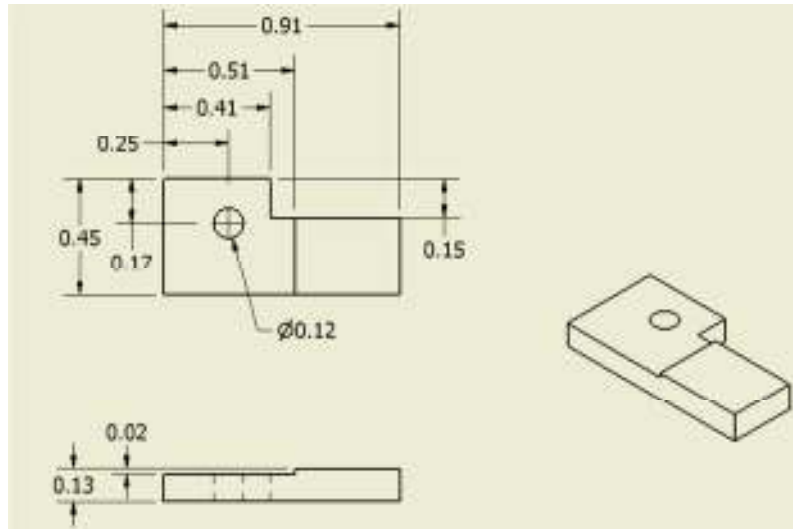


Figure 5.22 Front Left Plate

The front left plate has a rectangle cutout, 0.51 inch by 0.45 inch, and it is 0.02 inch deep. The plate is screwed to the front sensor block at the left-hand side through the clearance hole. A pressure sensor is stick to the thick rectangle surface and the top plate to measure the contact force.

Front Right Plate

Material: Aluminum 6061

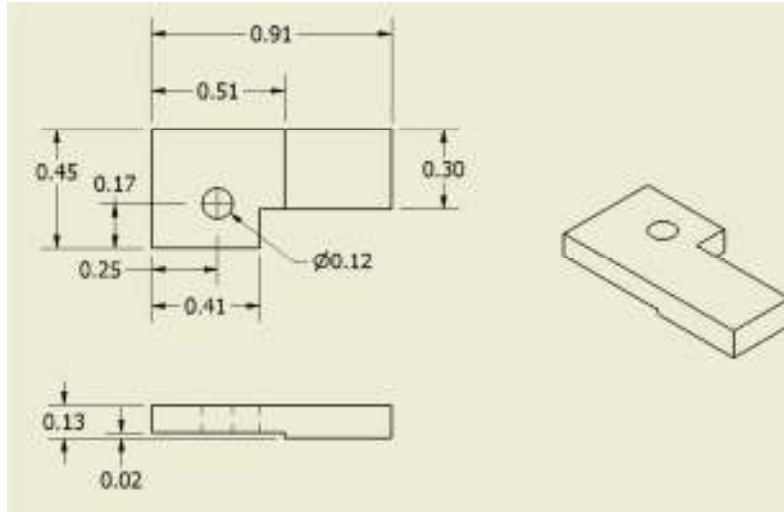


Figure 5.23 Front Right Plate

The front right plate has a clearance hole, and it is in same location compared to front left plate. The plate is screwed to the front sensor block through the clearance hole. The rectangle cutout has same dimension with cutout on the left plate, but it is on the opposite side of the plate.

Front Block

Material: Aluminum 6061

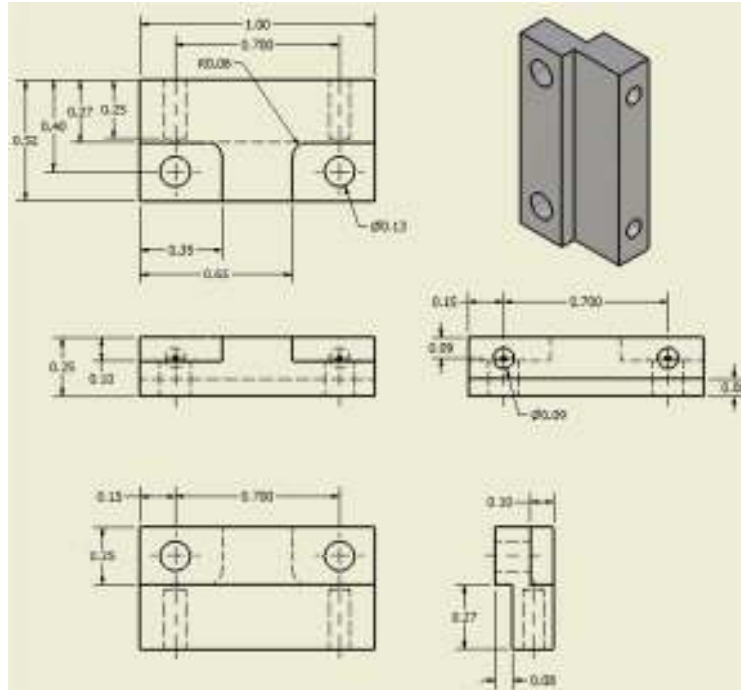


Figure 5.24 Front Block

The front block has two tapped holes and two clearance holes. The block is screwed to the bottom cover plate through clearance holes, and the front sensor block is fastened to block through tapped holes. A pressure sensor is stick to the top surface of the block to measure the contact force, and the front sensor block sits on the top of the sensor.

Back Block

Material: Aluminum 6061

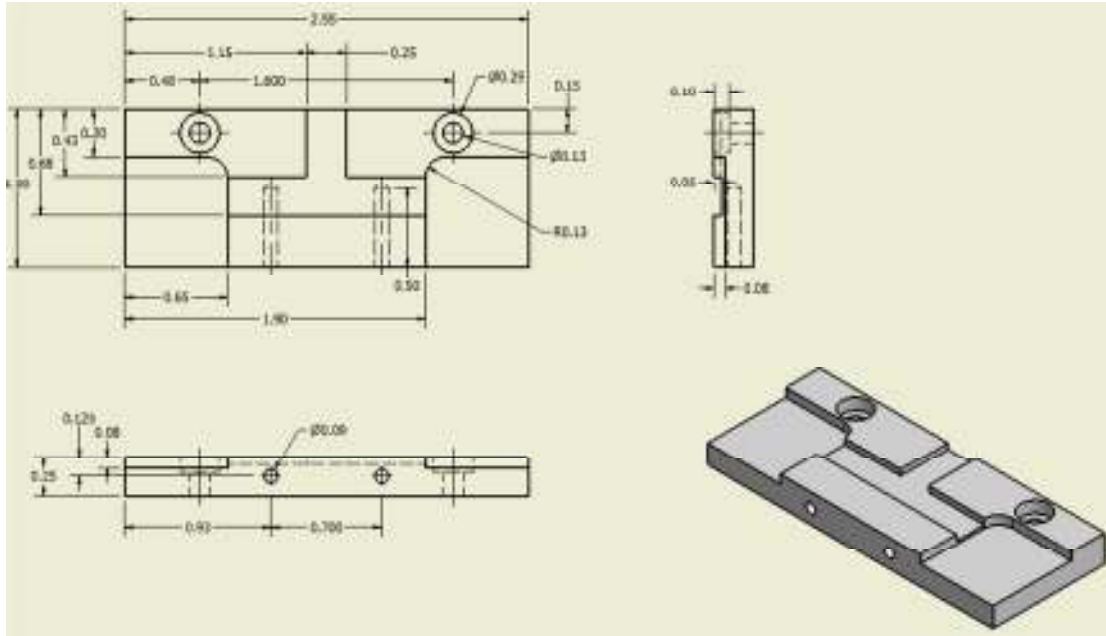


Figure 5.25 Back Block

The back block has two rectangle slots, and a T-shape slot. Pressure sensor is placed in each rectangle slot to measure contact force, and wires are passing through the T-shape slot. This block has two tapped holes, and two counterbores. The rear sensor block is screwed to the block through two tapped holes, and the block is fastened with the rear strain gage sensor block to the bottom cover plate through counterbores.

Front Strain Gage Sensor Block

Material: Aluminum 6061

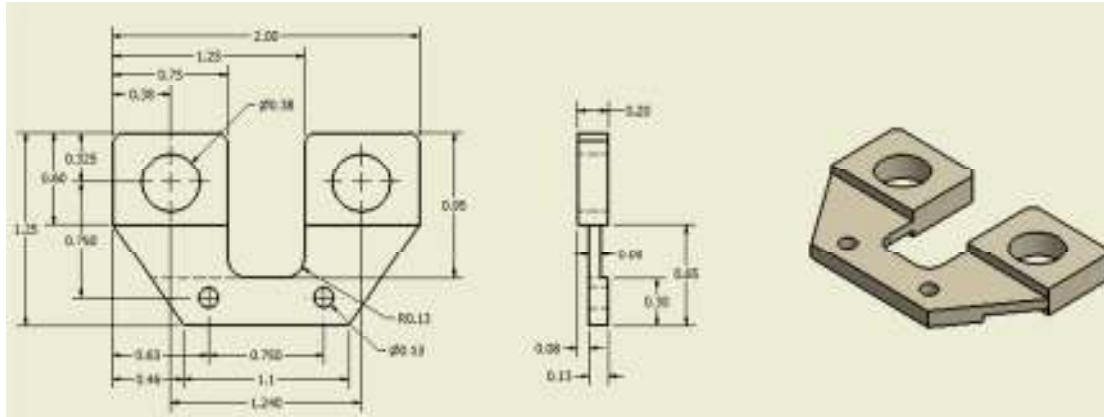


Figure 5.26 Front Strain Gage Sensor Block

The front strain gage sensor block has two large holes and two clearance holes. The block is screwed to the bottom cover plate through clearance holes. Torque sensors are assembled to large holes to measure input torques. Large holes are machined precisely so torque sensors would not wobble after assemble to these holes.

Rear Strain Gage Sensor Block

Material: Aluminum 6061

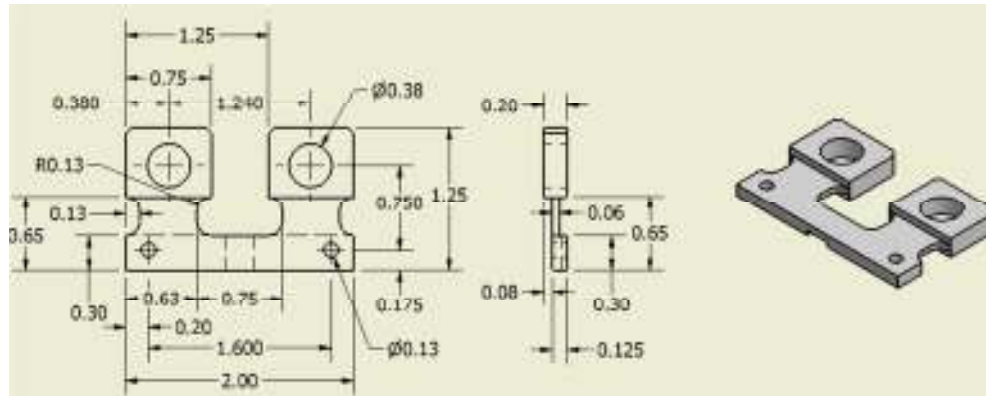


Figure 5.27 Rear Strain Gage Sensor Block

The rear strain gage sensor block has two clearance holes and two large holes. This block and the back block are fastened to the bottom cover plate through clearance holes. Two large holes are machined precisely so torque sensors would no wobble after assemble to these holes.

Bottom Cover Plate

Material: Aluminum 6061

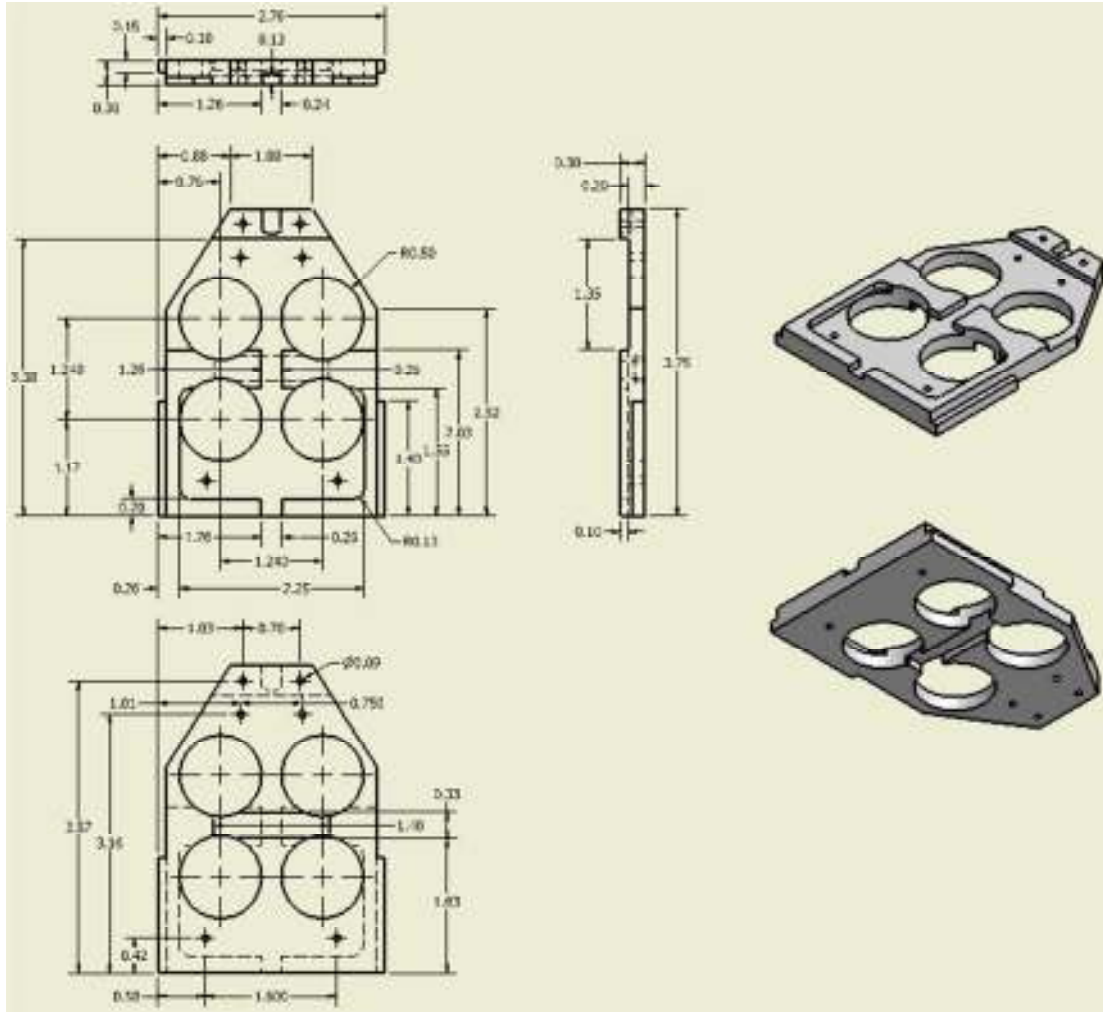


Figure 5.28 Bottom Cover Plate

The bottom cover plate is a complex design. The bottom surface of the plate has to fit to robotic arm adapter, and the rectangle slot allows the adapter to lock the plate to the robotic arm. Four large holes on the plate are aligned with torque sensors and the four large holes on the locking mechanism plate.

Top Wheel

Material: Aluminum 6061

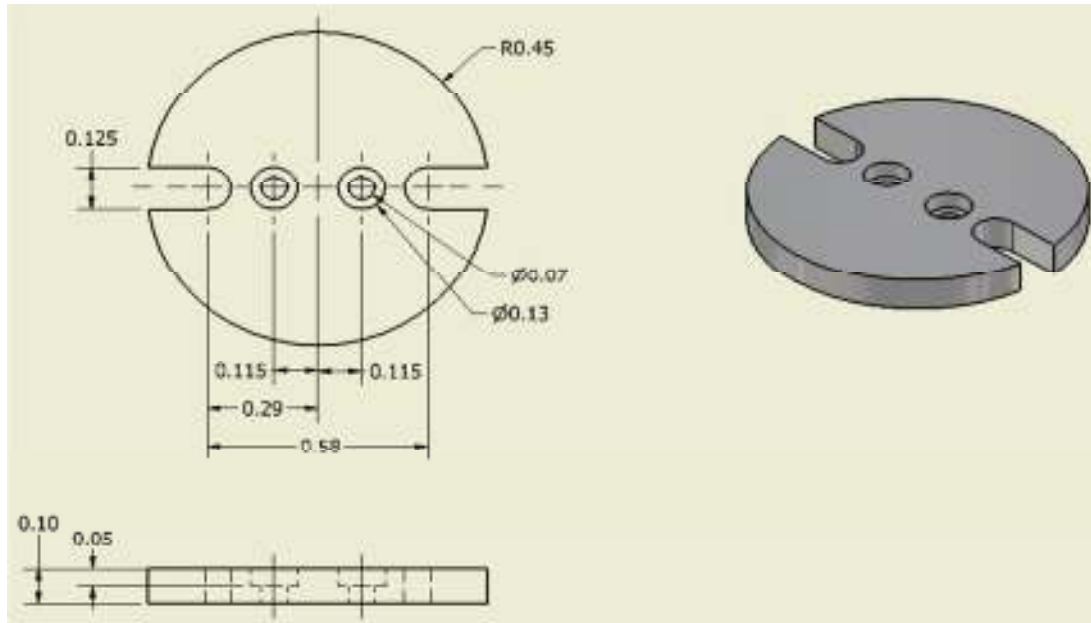


Figure 5.29 Top Wheel

The top wheel has two counterbores and two cutouts. The wheel is screwed to the support fixture through counterbores, and the cutouts fit to knobs on instrument wheels. When the top plate engages to instrument wheel, it could transfer input torque from the bottom wheel to the instrument wheel. The center of the wheel is aligned with the center of the large hole in the locking mechanism plate.

Bottom Wheel

Material: Aluminum 6061

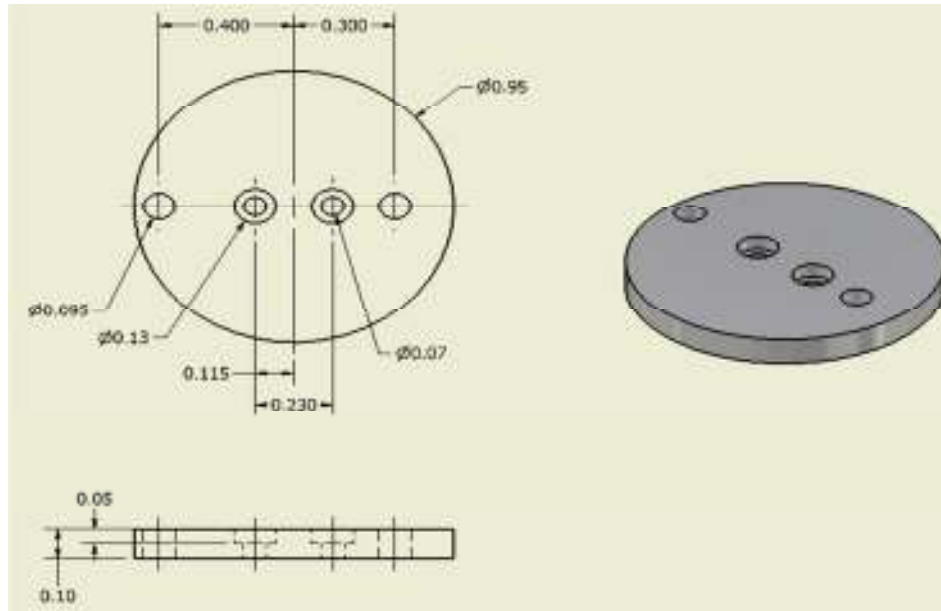


Figure 5.30 Bottom Wheel

The bottom wheel has two clearance holes and two counterbores. The wheel is screwed to the support fixture through counterbores. The diameter of the spring pin is 0.096 inch, and the compressed diameter is 0.093 inch. The clearance holes diameter has to be slightly larger than the compressed diameter so spring pins can fit into these holes.

Support Fixture

Material: Aluminum 6061

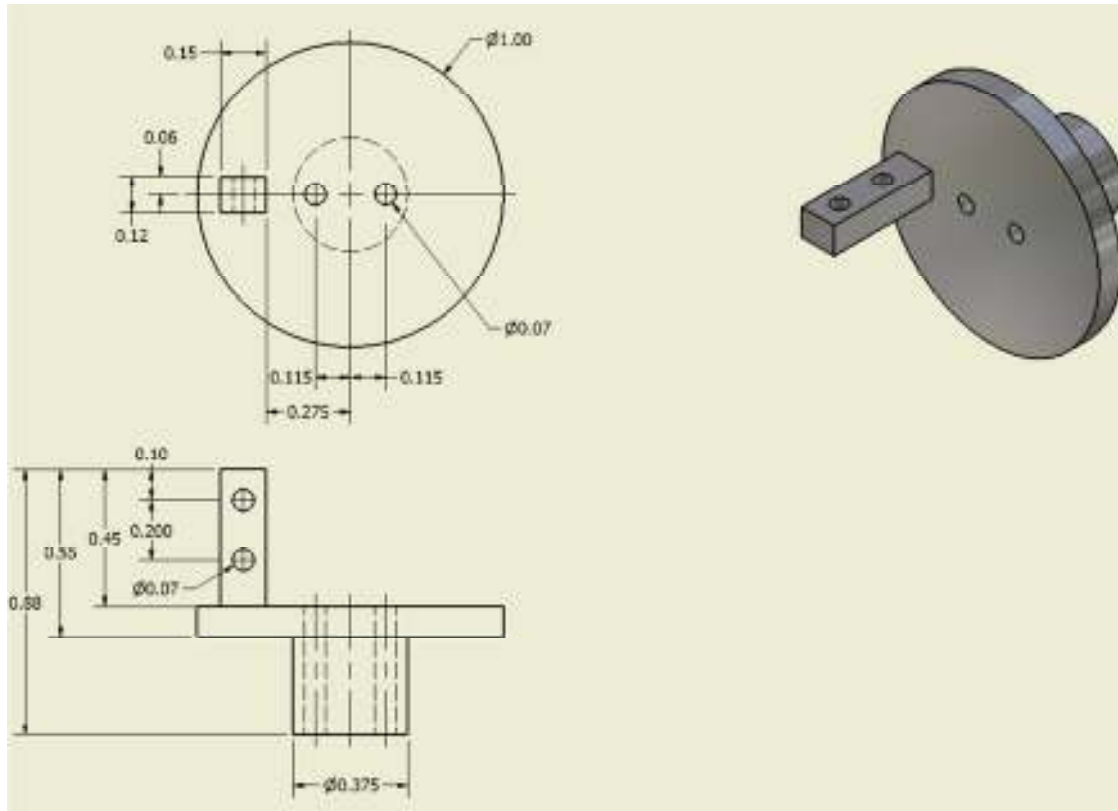


Figure 5.31 Support Fixture

The support fixture has two clearance holes and two tapped holes. One torque sensor has two support fixtures; one is screwed to the top wheel and the other one is fastened to the bottom wheel through clearance holes. The cantilever beam is screwed to both support fixtures through tapped holes. The bottom support fixture is assembled to the front strain gage sensor block or the rear strain gage sensor block, but top support fixture is not.

Cantilever Beam

Material: Aluminum 6061 Sheet Metal

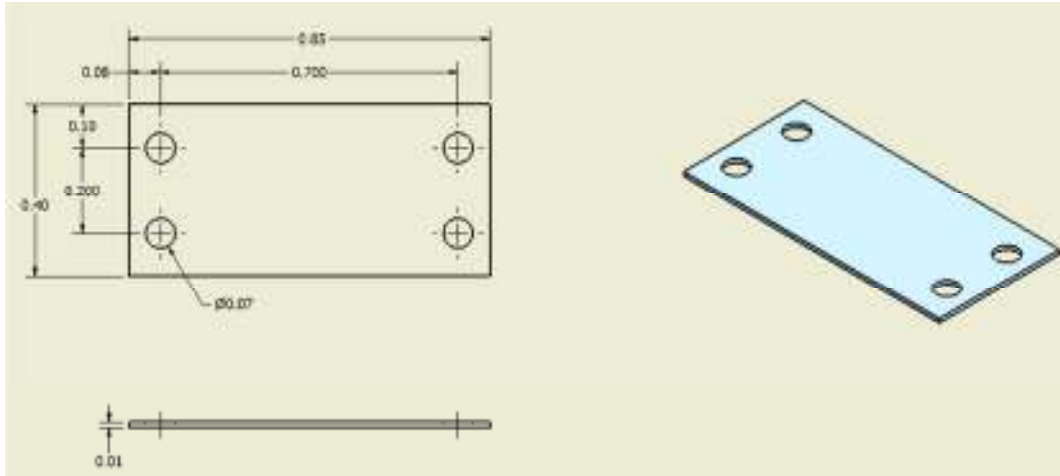


Figure 5.32 Cantilever Beam

The cantilever beam is made from aluminum sheet metal. The beam is screws to two support fixtures through these holes. A full-bridge strain gage is stick to the center of the beam to measure the input torque. The deflection of the cantilever beam depends on the input torque and the thickness of the beam. The thicker the beam is, the more torque can be transferred from robotic adapter wheels to instrument wheels.

Rear Side Block-Left

Material: Aluminum 6061

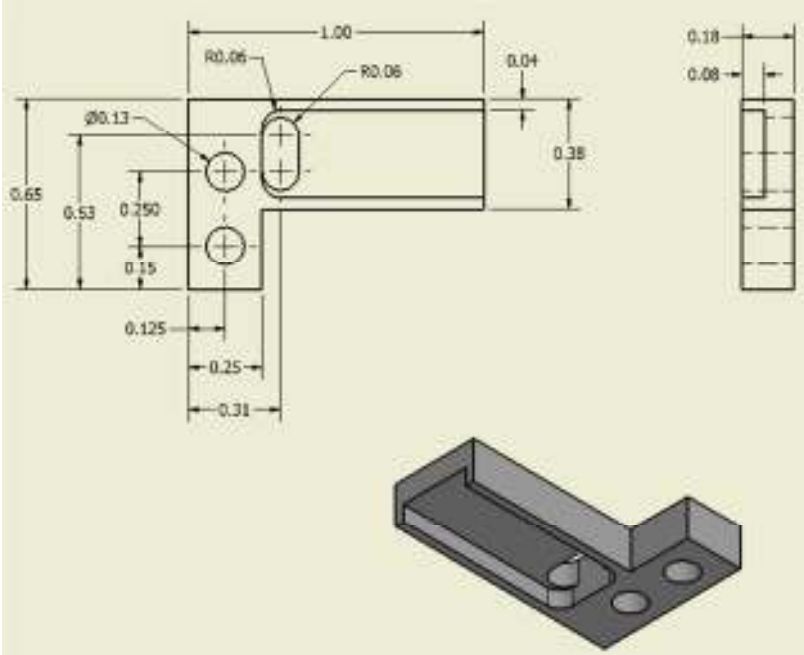


Figure 5.33 Left Rear Side Block

The block has two holes, one large rectangle slot and a round cutout. A pressure sensor is stick to the slot, and wires are passing through the round cutout. The block is screwed to the left-hand side of the rear sensor block, and the contact force between the block and the top plate can be measured utilizing the sensor.

Rear Side Block-Right

Material: Aluminum 6061 Sheet Metal

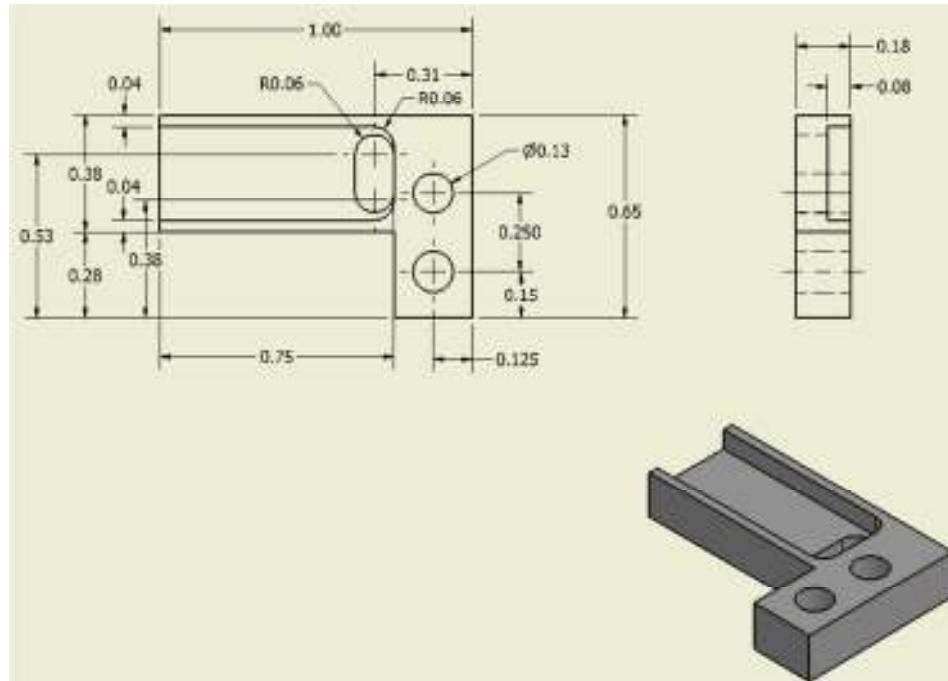


Figure 5.34 Right Rear Side Block

The block has two holes, a rectangle slot and a round cutout. A pressure sensor is stick to the rectangle slot to measure contact force between the block and the top plate, and sensor wires are passing through the round cutout. This block is screwed to the right-hand side of the rear sensor block.

Chapter 6 Prototype

Detailed drawings in the previous chapter show dimension of each component, and assembly drawings show how the sensor attachment is assembled together. Based on detailed drawings, parts can be manufactured in machine shop. Two machines are used to fabricate the prototype, lathe and milling machine. Parts must be machined utilizing lathe including, top wheel, bottom wheel and support fixture; other parts can be machined utilizing milling machine. Complex parts including, locking mechanism, locking mechanism plate, top cover plate, bottom cover plate, middle plate, support fixture, front strain gage sensor block and rear strain gage sensor block takes more time to fabricate.

6.1 Fabrication Results

All parts are manufactured in Stony Brook University machine shop.



Figure 6.1 Locking Mechanism Plate

The locking mechanism plate is made from a large and thick aluminum bar, 3 inch width and 0.63 inch thickness. The bar is cut to 4 inches long, and then clamped to the milling machine to take off some materials to achieve following dimension: 3.85 inch length, 3 inch width and 0.6 inch thickness. Rest of the machining work can be done utilizing milling machine,

and the work piece would look like the same as the one shown above. Other parts are done in similar way, and the machining process will not be described here.

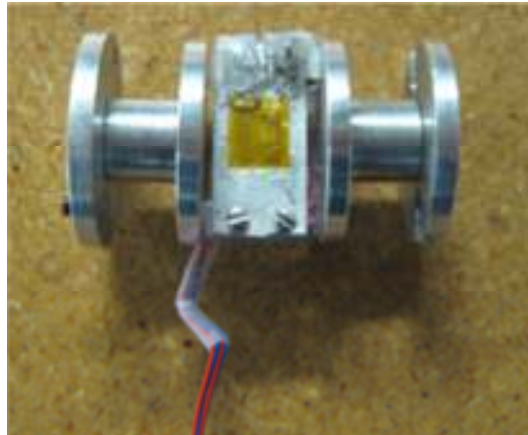


Figure 6.2 Torque Sensor Prototype

A full-bridge strain gage is mounted to the center of the cantilever beam to measure the input torque. The sensor has four wires; two wires are connecting to the battery and other two wires are connecting to a volt meter or the data acquisition to measure the voltage output while bending the cantilever beam.



Figure 6.3 Bottom Plate Installed to the Robot Adapter

The white plastic adapter in Figure 6.3 is removed from the Da Vinci robot arm. The bottom plate is fitted to the adapter very well; the finger tab on the adapter in the left-hand side of the picture inserted to the rectangle slot on the plate, and adapter wheels engage to torque sensors.

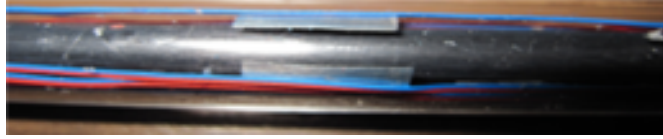


Figure 6.4 Instrument Shaft Inserted to Overcoat Tube

Sensors are stuck to the inner surface of overcoat tube. Wire clips are installed inside the tube to hold sensor wires and avoid damaging sensor while inserting the instrument shaft to the tube. In Figure 6.4, the shaft is inserted to the overcoat tube, and there is no contact between the shaft and the wire clip because of the gap.

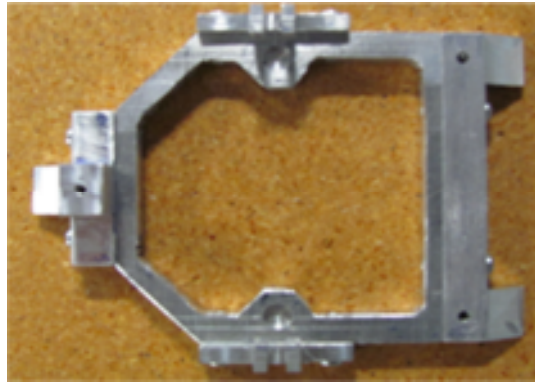


Figure 6.5 Middle Plate Assembly

In Figure 6.5, the front block, two side blocks and the rear middle block are assembled to the middle plate. There are two holes on the middle plate; springs are attached to the locking mechanism and then positioned to these two holes. The side block has a rectangle slot, and the locking mechanism moves inside the slot vertically.



Figure 6.6 Sensor Attachment with Endowrist Instrument

Figure 6.6 shows the Endowrist Instrument, the sensor attachment and the robot adapter are assembled together. The instrument is installed to the top plate, and the locking mechanism holds the instrument in position. By pressing the locking mechanism, the instrument adapter will be released from the top plate and then it can be removed from the sensor attachment. The picture shows the sensor attachment fits instrument and the robot adapter very well. There are many sensors installed to the sensor attachment, and many wires are exposed in the picture.

6.2 Circuitry

6.2.1 Sensor Circuits

A force sensing resistor is a sensor that changes resistance by applying force at the sensing area. As the load increases, the resistance decreases. It is in series with a resistor and is then connected to a battery. The voltage across the force sensing resistor decreases when the force applied to the sensing area increases.

Strain gages are connected with resistors to form a Wheatstone Bridge. Some circuits are half-bridge, and others are full-bridge. The half-bridge circuit measures the force parallel to the shaft, and the full bridge circuit measures the input torque. The output voltage from the Wheatstone Bridge is relatively small and utilizes an instrumentation amplifier to boost up the signal. NI USB 6225 is 16-bits data acquisition, and it is capable of measuring the output voltage directly from the Wheatstone Bridge circuit.

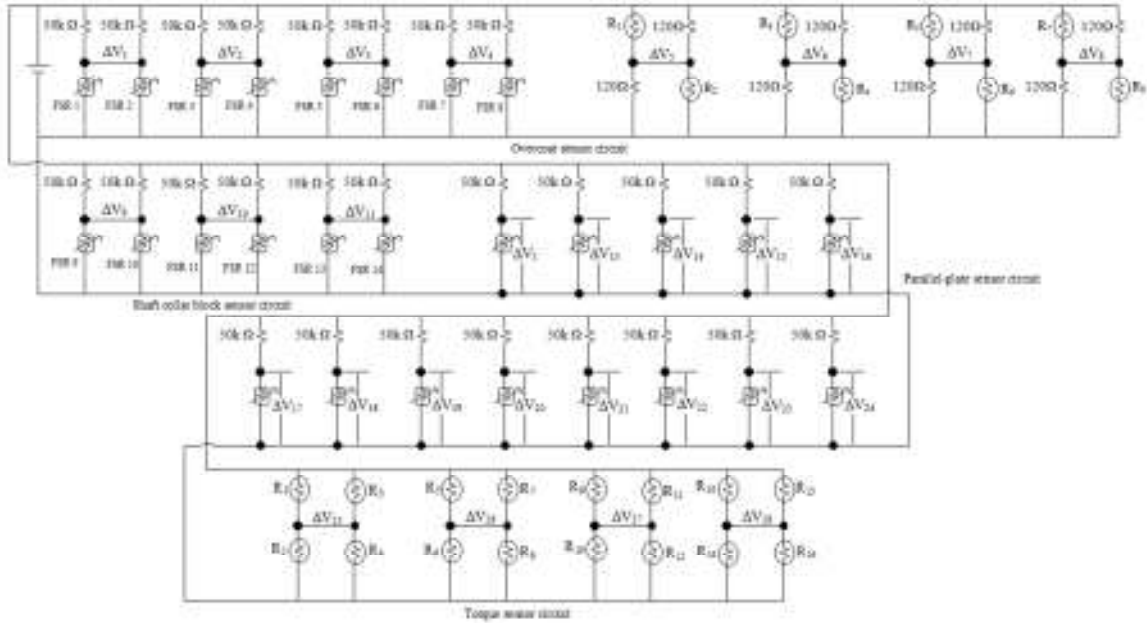


Figure 6.7 Sensor Circuit Diagram

First branch of the circuit diagram is the overcoat sensor circuit. Pressure sensor circuits are in the left-hand side and strain gage circuits are in the right-hand side. FSR1, FSR2, FSR3, FSR4, FSR5, FSR6, FSR7 and FSR8 are pressure sensors. R1, R2, R3, R4, R5, R6, R7 and R8 are 120 ohm strain gages. FSR1, FSR2, FSR3, FSR4, R1, R2, R3 and R4 are located at the front of the tube. FSR1 and R1 are stuck to the top, FSR2 and R2 are stuck to the bottom, FSR3 and R3 are stuck to the left, FSR4 and R4 are stuck to the right. FSR5, FSR6, FSR7, FSR8, R5, R6, R7 and R8 are located at the rear of the tube. FSR5 and R5 are stuck to the top, FSR6 and R6 are stuck to the bottom, FSR7 and R7 are stuck to the left, FSR8 and R8 are stuck to the right. When applying force, if FSR1 resistance increases, then FSR2 resistance decreases. Pressure sensors are facing opposite to each other will work the same way; if one sensor resistance increases, then the other sensor resistance decreases. Resistance of strain gages are increases or decrease at the same time when applying force parallel to the tube.

Pressure sensors are installed to shaft collar plate and the overcoat block to measure contact forces between the shaft collar and the sensor attachment adapter. Shaft collar block sensor circuit is shown in the second branch left-hand side of the circuit diagram. FSR9, FSR11 and FSR13 are located on one side of the shaft collar, and FSR10, FSR12 and FSR14 are located on the other side of the shaft collar. If FSR9 resistance increases, then FSR11 resistance decreases. Pressure sensors are facing opposite to each other works just like the overcoat pressure sensors.

Pressure sensors are stuck to every contact point between the top plate and the bottom plate. The sensor is in series with a resistor and connects to the battery. When applying force to the sensing area of the sensor, the resistance decreases. The second branch right-hand side circuits and the third branch circuits are parallel-plate circuits.

Torque sensor circuits are shown in the last branch of the circuit diagram. A full-bridge strain gage is stuck to the torque sensor cantilever beam to measure the input torque. The sensor has four wires; two wires are connecting to the battery, and other two wires are connecting to data acquisition to measure the voltage output.

6.2.2 PCB Board Circuits

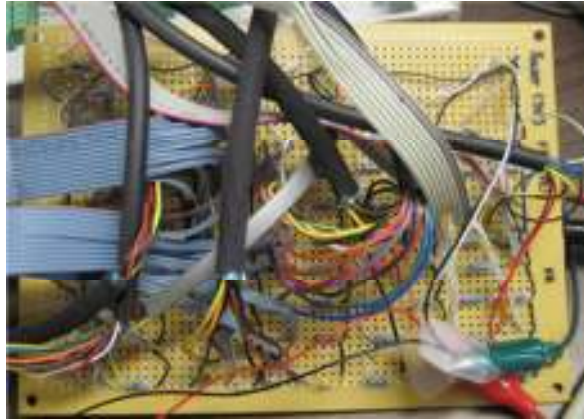


Figure 6.8 PCB Board A

Most circuits are soldered to PCB board A; there are many resistors and wires are soldered to the board in Figure 6.8. Two alligator clips are hooked up to four wires; red alligator clip clamped to the white and red wires, and the green alligator clip clamped to two black wires. Both clips are connecting to the power supply; red clip connects to positive and green clip connects to negative. Circuit output is hooked up to the data acquisition to do the calibration.

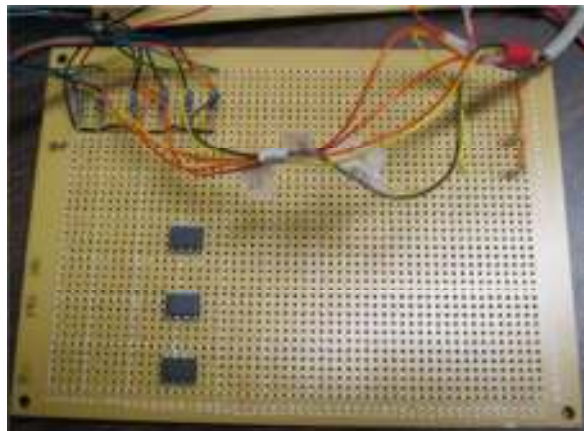


Figure 6.9 PCB Board B

Remaining circuits are soldered to PCB board B. In Figure 6.9, there are few resistors and wires. Instrument amplifiers are soldered to the board, but these amplifiers are useless because the data acquisition is capable of measuring voltage output from Wheatstone Bridge directly. The power supply provides power to both, PCB board A and B.

Chapter 7 Experimental Setup

Endowrist Instrument is installed to the sensor attachment, and torque sensors are engaged to instrument wheels. Force machine and torque machine are required to calibrate the sensor attachment; force machine measures the instrument tip force and the torque machine measures the input torque. The torque machine in the lab only measures one input torque, so the calibration has to be done in another way.

7.1 Aluminum Frame



Figure 7.1 Aluminum Frame

Aluminum frame is required to hold the sensor attachment and do the calibration. Four cylinders are screwed to a large rectangle plate, and four aluminum bars are fastened to the top of cylinders. The finger tab is screwed to the front bar and two blocks are installed to side bars to

hold the sensor attachment to the frame. Cylinders are long enough to give excess space to install the sensor attachment. The frame can be adjusted to move closer or move away from the torque machine. In Figure 7.1, the frame is clamped to the torque machine and it is adjustable to satisfy experimental requirements.



Figure 7.2 Adjust Frame Length

The length of the aluminum frame can be adjusted. In Figure 7.2, the bar at the left-hand side has a long rectangle slot that allows the bar to move horizontally. The block above it has two tapped holes, and the aluminum bar at the right-hand side has two clearance holes. Two screws are passing through clearance holes on the right-hand side aluminum bar and fastened to the aluminum block to hold both bars tight. The length of the frame can be adjusted by losing these two screws with a screw driver. The wheel mechanism at the left hand side can be adjusted to apply three-dimensional forces to the tip of the instrument.

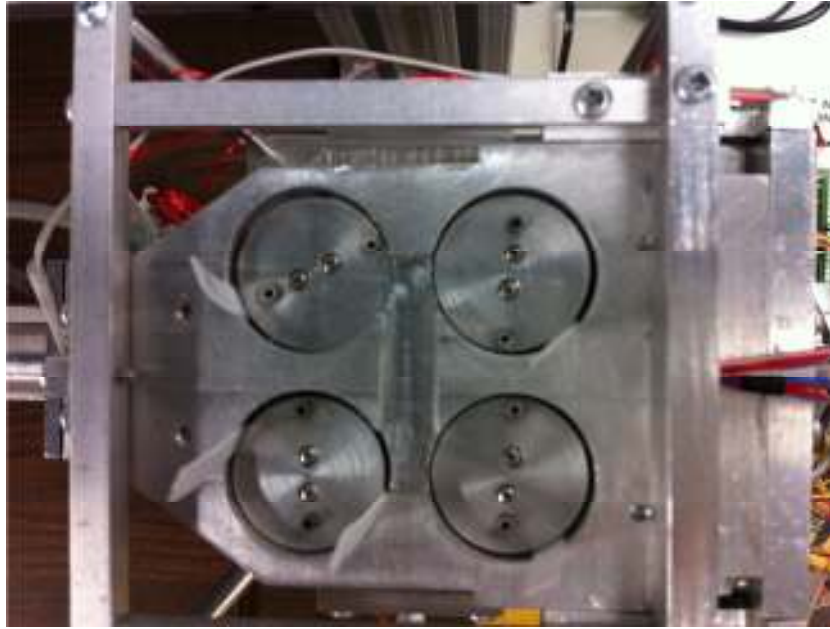


Figure 7.3 Plastic Strips Inserted to Sensor Attachment

Four plastic strips are inserted to the gap between the bottom wheel and the large hole on the bottom cover plate to limit the rotation of the torque sensor. Bottom wheels are fixed; torque sensor cantilever beams bend by applying force to the tip of the instrument. Utilizing this method, no commercial torque sensors are necessary to measure input torques.



Figure 7.4 Sensor Attachment Installed to Aluminum Frame

In the figure shown above, the force machine is in the left-hand side, and the torque machine is in the right-hand side. The force machine has few buttons to control vertical movement of the force gage. A string is tied to the tip of the instrument and hanged to the force gage hook. When pressing UP button, force gage moves up; it applies force to the tip of the instrument and measures the tip force at the same time.



Figure 7.5 Calibrate Tip Force in X-Axis

In Figure 7.5, a string is tied to the tip of the instrument and hanged to the force gage hook vertically. When pressing the UP button on the force machine, the force gage moves up and pulls the string. As a result, force is applied to the tip of the instrument and it is measured utilizing force gage. The sensor attachment x-axis force can be calibrated utilizing this method.



Figure 7.6 Calibrate Tip Force in Y-Axis

The wheel mechanism on the frame rotated 90 degrees counter clockwise. The string is tied to the tip of the instrument and wrapped around the wheel, and then hanged to the force gage hook. Force is applied to the instrument tip in y-axis by moving the force gage upward.

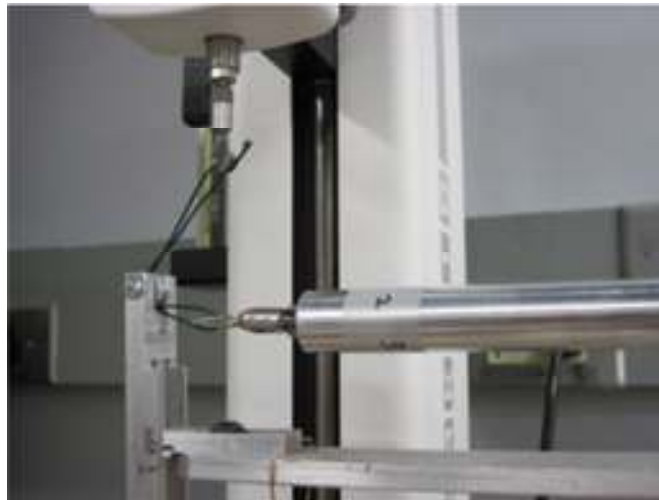


Figure 7.7 Calibrate Tip Force in Z-Axis

In Figure 7.7, the wheel mechanism is rotated 90 degrees clockwise. The string is tied to the instrument tip and wrapped around the wheel, and then hanged to the force gage hook. Force is applied to the tip of the instrument in z-axis by moving the force gage upward.

7.2 Signal Processing

Sensor wires are soldered to PCB boards, and the power supply delivers power to the circuit. Data acquisition is connected to the PCB board to acquire data, and it then sends the signal to the computer. Signal Express is used to acquire data, and the calibration can be done utilizing LabVIEW. The diagram is shown below:

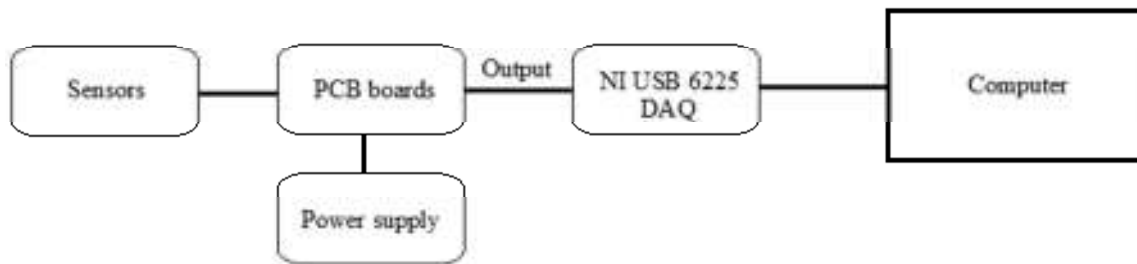


Figure 7.8 Signal Processing Diagram

7.3 Calibration Equations

The relationship between the voltage output and the force is linear, and the equation is shown below:

$$F = C \cdot (V - V_0) \tag{7.3.1}$$

where C is the coefficient, V is the sensor measurement, and V_0 is the initial voltage.

X-axis force calibration equation is listed below:

$$F_{7x} = C_{4x} \cdot (V_{4x} - V_{40x}) + C_{5x} \cdot (V_{5x} - V_{50x}) + C_{9x} \cdot (V_{9x} - V_{90x}) + C_{17x} \cdot (V_{17x} - V_{170x}) + C_{18x} \cdot (V_{18x} - V_{180x}) \quad 7.3.2$$

When calibrating the force at the tip of instrument, the weight of the instrument and the top plate are already taken into consideration.

X-axis moment calibration equation is listed below:

$$M_{7x} = B_{4y} \cdot (V_{4y} - V_{40y}) + B_{4z} \cdot (V_{4z} - V_{40z}) + B_{5y} \cdot (V_{5y} - V_{50y}) + B_{5z} \cdot (V_{5z} - V_{50z}) + B_{61z} \cdot (V_{61z} - V_{610z}) + B_{62z} \cdot (V_{62z} - V_{620z}) + B_{63z} \cdot (V_{63z} - V_{630z}) + B_{8y} \cdot (V_{8y} - V_{80y}) + B_{9z} \cdot (V_{9z} - V_{90z}) + B_{10y} \cdot (V_{10y} - V_{100y}) + B_{16y} \cdot (V_{16y} - V_{160y}) + B_{17z} \cdot (V_{17z} - V_{170z}) + B_{18z} \cdot (V_{18z} - V_{180z}) + B_{19y} \cdot (V_{19y} - V_{190y}) + B_{11x} \cdot (V_{11x} - V_{110x}) + B_{12x} \cdot (V_{12x} - V_{120x}) + B_{14x} \cdot (V_{14x} - V_{140x}) + B_{15x} \cdot (V_{15x} - V_{150x}) \quad 7.3.3$$

Y-axis force calibration equation is listed below:

$$F_{7y} = C_{4y} \cdot (V_{4y} - V_{40y}) + C_{5y} \cdot (V_{5y} - V_{50y}) + C_{8y} \cdot (V_{8y} - V_{80y}) + C_{10y} \cdot (V_{10y} - V_{100y}) + C_{16y} \cdot (V_{16y} - V_{160y}) + C_{19y} \cdot (V_{19y} - V_{190y}) \quad 7.3.4$$

Z-axis force calibration equation is listed below:

$$F_{7z} = C_{4z} \cdot (V_{4z} - V_{40z}) + C_{5z} \cdot (V_{5z} - V_{50z}) + C_{61z} \cdot (V_{61z} - V_{610z}) + C_{62z} \cdot (V_{62z} - V_{620z}) + C_{63z} \cdot (V_{63z} - V_{630z}) + C_{9z} \cdot (V_{9z} - V_{90z}) + C_{17z} \cdot (V_{17z} - V_{170z}) + C_{18z} \cdot (V_{18z} - V_{180z}) \quad 7.3.5$$

7.4 LabVIEW Programming

Data can be acquired utilizing Signal Express and coefficients can be calculated by using MatLAB. After this, create a LabVIEW program, and then enter coefficients to calibrate the sensor attachment.



Figure 7.9 LabVIEW Front Panel

The front panel has four gauges, three force gauges and one moment gauge. Force gauges measure three-component forces at the tip of the instrument, and the moment gauge measures the moment about x-axis. The program will run by clicking the RUN button and it stops when clicking the STOP button.

The block diagram shown below is for calibrating the sensor attachment. The top left-hand side of the program is used to calibrate forces in x-axis, and the top right-side program is used to calibrate forces in y-axis. In a similar manner, the bottom-left program is used to calibrate z-axis force, and the program at the bottom right is used to calibrate the moment about the x-axis.

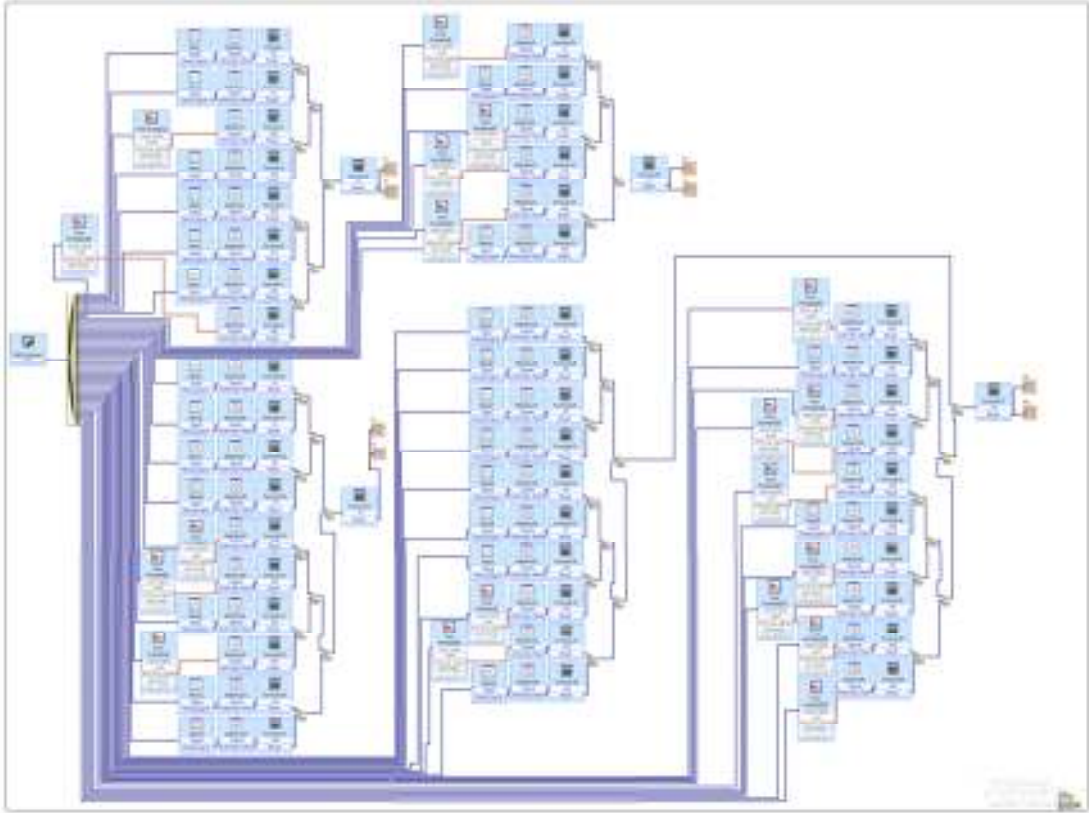


Figure 7.10 LabVIEW Block Diagram

Chapter 8 Results and Discussion

Three-dimensional forces are applied to the tip of the instrument and can be measured utilizing the force gage and the sensor attachment. Applied force is measured by the force gage, and the calibrated force is measured by the sensor attachment. Experiment is repeated three times; applied force is same and only measured once, but the calibrated force is measured three times. The mean of the calibrated force measurements are calculated based on three trials force measurement and the error can be determined.

8.1 Results

Applied Force (lbf)	Trial 1	Trial 2	Trial 3	Mean	% Error
0.20	0.19	0.18	0.18	0.18	8.33
0.22	0.23	0.22	0.21	0.22	0.00
0.24	0.24	0.25	0.25	0.25	2.78
0.26	0.25	0.28	0.28	0.27	3.85
0.28	0.28	0.31	0.30	0.30	5.95
0.30	0.31	0.34	0.33	0.33	8.89
0.32	0.33	0.35	0.36	0.35	8.33
0.34	0.37	0.35	0.36	0.36	5.88
0.36	0.38	0.36	0.37	0.37	2.78
0.38	0.39	0.37	0.37	0.38	0.88
0.40	0.39	0.39	0.40	0.39	1.67
0.42	0.40	0.40	0.43	0.41	2.38
0.44	0.41	0.42	0.44	0.42	3.79
0.46	0.44	0.47	0.46	0.46	0.72
0.48	0.47	0.49	0.47	0.48	0.69
0.50	0.48	0.49	0.49	0.49	2.67
0.52	0.50	0.52	0.51	0.51	1.92
0.54	0.52	0.54	0.54	0.53	1.23
0.56	0.56	0.57	0.56	0.56	0.60
0.58	0.59	0.58	0.57	0.58	0.00
0.60	0.62	0.60	0.60	0.61	1.11
0.62	0.64	0.64	0.63	0.64	2.69
0.64	0.67	0.66	0.66	0.66	3.65
0.66	0.69	0.68	0.69	0.69	4.04
0.68	0.70	0.70	0.71	0.70	3.43
0.70	0.72	0.71	0.73	0.72	2.86
0.72	0.76	0.73	0.74	0.74	3.24
0.74	0.76	0.75	0.77	0.76	2.70
0.76	0.76	0.77	0.78	0.77	1.32
0.78	0.77	0.80	0.79	0.79	0.85
0.80	0.79	0.81	0.80	0.80	0.00
0.82	0.81	0.83	0.80	0.81	0.81
0.84	0.83	0.85	0.83	0.84	0.40
0.86	0.86	0.88	0.85	0.86	0.39
0.88	0.89	0.89	0.87	0.88	0.38
0.90	0.90	0.92	0.90	0.91	0.74
0.92	0.91	0.93	0.92	0.92	0.00
0.94	0.93	0.95	0.92	0.93	0.71
0.96	0.96	0.96	0.94	0.95	0.69
0.98	0.98	0.97	0.96	0.97	1.02
1.00	0.99	1.00	0.98	0.99	1.00

Table 8.1 X-axis Force Measurements

Force range in x-axis is from 0.20 pound to 1.00 pound, and the force increment is 0.02 pound. The first column is the applied force measured utilizing the force gage. The second, third and fourth columns are three trials force measurements measured by the sensor attachment.

The mean can be calculated by taking average of three trials force measurements. The error can be determined by comparing the applied force and the mean. According to Table 8.1, error stabilized when the applied force exceeds 0.34 pound, and the precision of sensors is 0.03 pound force.

Applied Force (lbf)	Trial 1	Trial 2	Trial 3	Mean	% Error
0.20	0.20	0.23	0.20	0.21	5.00
0.22	0.22	0.24	0.22	0.23	3.03
0.24	0.24	0.25	0.25	0.25	2.78
0.26	0.26	0.28	0.27	0.27	3.85
0.28	0.28	0.29	0.28	0.28	1.19
0.30	0.29	0.30	0.29	0.29	2.22
0.32	0.31	0.32	0.30	0.31	3.13
0.34	0.32	0.33	0.32	0.32	4.90
0.36	0.34	0.35	0.34	0.34	4.63
0.38	0.38	0.37	0.36	0.37	2.63
0.40	0.40	0.39	0.38	0.39	2.50
0.42	0.42	0.41	0.40	0.41	2.38
0.44	0.44	0.42	0.41	0.42	3.79
0.46	0.46	0.44	0.44	0.45	2.90
0.48	0.47	0.45	0.46	0.46	4.17
0.50	0.49	0.48	0.48	0.48	3.33
0.52	0.50	0.50	0.50	0.50	3.85
0.54	0.53	0.53	0.53	0.53	1.85
0.56	0.55	0.55	0.55	0.55	1.79
0.58	0.58	0.57	0.58	0.58	0.57
0.60	0.60	0.60	0.60	0.60	0.00
0.62	0.61	0.61	0.62	0.61	1.08
0.64	0.63	0.63	0.64	0.63	1.04
0.66	0.65	0.65	0.67	0.66	0.51
0.68	0.67	0.67	0.68	0.67	0.98
0.70	0.68	0.68	0.69	0.68	2.38

Table 8.2 Y-axis Force Measurements

Force range in y-axis is from 0.20 pound to 0.70 pound, and the force increment is 0.02 pound. According to Table 7.2, the maximum error occurs when the applied force is minimum. The applied force is 0.20 pound, and the mean is 0.21 pound; even though the difference between these two forces is small, however it contributes the maximum error of 5 percent. The

precision of sensors is 0.02 pound force, so the applied force starts from 0.20 pound in order to have error within 10 percent.

Applied Moment (lb-in)	Trial 1	Trial 2	Trial 3	Mean	% Error
0.40	0.38	0.45	0.43	0.42	5.00
0.44	0.42	0.48	0.46	0.45	3.03
0.48	0.47	0.51	0.50	0.49	2.78
0.52	0.50	0.55	0.53	0.53	1.28
0.56	0.54	0.59	0.56	0.56	0.60
0.60	0.59	0.62	0.60	0.60	0.56
0.64	0.62	0.66	0.63	0.64	0.52
0.68	0.66	0.70	0.67	0.68	0.49
0.72	0.70	0.74	0.71	0.72	0.46
0.76	0.76	0.79	0.77	0.77	1.75
0.80	0.81	0.84	0.83	0.83	3.33
0.84	0.85	0.88	0.87	0.87	3.17
0.88	0.90	0.92	0.91	0.91	3.41
0.92	0.95	0.96	0.97	0.96	4.35
0.96	1.00	1.01	1.02	1.01	5.21
1.00	1.04	1.06	1.06	1.05	5.33
1.04	1.08	1.12	1.11	1.10	6.09
1.08	1.13	1.17	1.15	1.15	6.48
1.12	1.16	1.20	1.20	1.19	5.95
1.16	1.22	1.25	1.25	1.24	6.90
1.20	1.25	1.29	1.29	1.28	6.39
1.24	1.29	1.33	1.33	1.32	6.18
1.28	1.34	1.37	1.37	1.36	6.25
1.32	1.37	1.41	1.40	1.39	5.56
1.36	1.40	1.44	1.44	1.43	4.90
1.40	1.43	1.49	1.49	1.47	5.00

Table 8.3 Moment about X-Axis

Force applied to the tip of the instrument in y-axis can be used to calculate the applied moment about the x-axis. The y-axis force multiplied a constant equals to the moment. Moment about x-axis is range from 0.40 pound inch to 1.40 pound inch, and the increment is 0.04 pound inch. According to Table 7.3, large error occurs when the moment exceeds 0.92 pound inch. The maximum error is less than 10 percent, and it is acceptable.

Applied Force (lbf)	Trial 1	Trial 2	Trial 3	Mean	% Error
0.28	0.27	0.26	0.30	0.28	1.19
0.32	0.30	0.30	0.35	0.32	1.04
0.36	0.35	0.39	0.39	0.38	4.63
0.40	0.38	0.42	0.46	0.42	5.00
0.44	0.44	0.48	0.49	0.47	6.82
0.48	0.51	0.52	0.54	0.52	9.03
0.52	0.53	0.56	0.58	0.56	7.05
0.56	0.55	0.58	0.61	0.58	3.57
0.60	0.59	0.63	0.63	0.62	2.78
0.64	0.63	0.67	0.67	0.66	2.60
0.68	0.69	0.74	0.74	0.72	6.37
0.72	0.74	0.77	0.79	0.77	6.48
0.76	0.77	0.82	0.82	0.80	5.70
0.80	0.80	0.85	0.85	0.83	4.17
0.84	0.84	0.88	0.89	0.87	3.57
0.88	0.86	0.90	0.90	0.89	0.76
0.92	0.89	0.92	0.93	0.91	0.72
0.96	0.92	0.94	0.96	0.94	2.08
1.00	0.96	0.99	0.99	0.98	2.00
1.04	1.00	1.06	1.06	1.04	0.00
1.08	1.05	1.11	1.11	1.09	0.93
1.12	1.10	1.15	1.13	1.13	0.60
1.16	1.14	1.17	1.18	1.16	0.29
1.20	1.16	1.20	1.21	1.19	0.83
1.24	1.19	1.23	1.23	1.22	1.88
1.28	1.22	1.26	1.26	1.25	2.60
1.32	1.26	1.28	1.29	1.28	3.28

Table 8.4 Z-Axis Force Measurements

Force in z-axis is range from 0.28 pound to 1.32 pound, and the force increment is 0.04 pound. According to Table 7.4, maximum error occurs when the applied force is 0.48 pound, and the mean is 0.52 pound. The error is stabilized when the applied force exceed 0.76 pound.

8.2 Discussion

The force range in x-axis is from 0.20 pound to 1.00 pound, the force range in y-axis is from 0.20 pound to 0.70 pound, the moment about x-axis range from 0.40 pound inch to 1.40 pound inch and the force range in z-axis is from 0.28 pound to 1.32 pound. The force range and moment range can be improved by changing the torque sensor cantilever beam to thicker beam. Thicker cantilever beam allows transferring more torque from the robot arm adapter wheels to instrument wheels. So larger force can be applied to the tip of the instrument, and the error can be reduced.

The force gage precision is 0.002 pound force, but the force increment in x-axis and y-axis is 0.02 pound force, and the force increment in z-axis is 0.04 pound force. The reason for this is the pressure sensor inside the sensor attachment has force error up to 25 percent. If the force increment is less than 0.02 pound, then the sensor attachment will be difficult to calibrate. The precision of the sensor attachment can be improved by using more accurate sensors.

A full-bridge strain gage is stuck to the torque sensor cantilever beam to measure the input torque. The strain gage has four wires, and wires are wrapping around the torque sensor. Wires can be pulled off from the strain gage by rotating the torque sensor. To solve this problem, the torque sensor needs to be redesigned.

The strain gage and the pressure sensor are stuck between two pieces of rubber, and then glued to the inner surface of the tube. It is difficult to stick sensors to the inner surface of the tube, and the rubber is hardened when the glue is dried. If the glue sticks to the pressure sensor while gluing the sensor to the tube, then the pressure sensor would be damaged when inserting the instrument shaft to the tube. In addition, wire clips are difficult to insert to the tube.

Chapter 9 Conclusion and Future Work

9.1 Conclusion

The sensor attachment is designed to fit Endowrist Instrument and robot adapter. Sensors are stuck to then rubber, and then glued to the inner surface of the tube, so there is no gap when inserting the instrument shaft to the tube, due to the flexibility of the rubber. There are different types instrument in the market and the major difference is the tip, but the shaft diameter is same. All instruments would fit when inserting to the overcoat tube. The tube is connecting to the sensor adapter through the shaft collar, and the sensor inside the shaft collar block measures the supporting force on the shaft collar.

The top plate is designed to fit any Endowrist Instrument. When inserting the instrument to the top plate, the locking mechanism would lock the instrument to the top plate automatically. To remove the instrument, press on the locking mechanism to unlock the instrument, and then take out the instrument from the sensor attachment. The top plate is clamped to the bottom plate, and sensors are placed between the top plate and bottom plate to measure the contact force between the instrument adapter and the robot adapter.

The bottom plate is designed to fit the robot adapter. The bottom plate has a rectangle groove, which allows the robot adapter to lock the sensor attachment to the robot arm. Front strain gage sensor block and rear strain gage sensor block are screwed to the bottom cover plate, and torque sensors are installed to these two blocks to measure input torque.

The sensor attachment solved most problems that appear in existing sensor designs and some problems that have not been discovered by other people. Furthermore, another problem has been discovered, but there is no solution yet. The compression force at the tip of the instrument cannot be measured with existing sensors designs.

9.2 Future Work

The sensor attachment measures three-dimensional forces at the tip of the instrument and input torques. However, the compression force at the tip cannot be measured. The compression forces on both grippers have the same magnitude but act in opposite directions. As a result of this, the force is cancelled out in the total force equation. Furthermore, there is a linear relationship between the compression force at the tip and the input torque, and the equation can be derived.

When the instrument shaft rotates, overcoat the tube rotates at the same direction as well. The rotational angle has to be measured if the shaft is free to rotate, otherwise the force perpendicular to the shaft cannot be calibrated accurately. The strain gage is mounted to the torque sensor cantilever beam, and wires are wrapped around the beam when rotating the torque sensor. So, the torque sensor design needs to be improved in order to eliminate this problem. In addition, an acceleration sensor is required to measure the dynamic force.

Reference

1. R Bauernschmitt, E U Schirmbeck, A Knoll, H Mayer, I Nagy, N Wessel, S M Wildhirt, R Lange. Towards robotic heart surgery: Introduction of autonomous procedures into an experimental surgical telemanipulator system 2005; 1(3):74-79.
2. S. Shimachi, Y. Hakozaiki, T. Tada, Y. Fujiwara. Measurement of force acting on surgical instrument for force-feedback to master robot console (2003) 538-546.
3. S. Shimachi, Y. Fujiwara, Y. Hakozaiki. New sensing method of force acting on instrument for laparoscopic robot surgery (2004) 775-780.
4. Shigeyuki Shimachi, Surakij Hirunyanitiwatna, Yasunori Fujiwara, Akira Hashimoto, Yoshinori Hakozaiki. Adapter for contact force sensing of the da Vinci robot 2008, 4: 121-130.
5. Shigeyuki Shimachi, Fumie Kameyama, Yoshihide Hakozaiki, Yasunori Fujiwara. Contact force measurement of instruments for force-feedback on a surgical robot: Acceleration force cancellations based on acceleration sensor readings. pp. 97-104 (2005).
6. Nabil Zemiti, Tobias Ortmaier, Guillaume Morel. A new robot for force control in minimally invasive surgery. IEEE/RSJ International Conference on Intelligent Robots and Systems, pp.3643-3648, 2004.
7. Tamas Haidegger, Balazs Benyo, Levente Kovacs, Zoltan Benyo. Force sensing and force control for surgical robots. Proceedings of the 7th IFAC Symposium on Modelling and Control in Biomedical Systems, pp.413-418, 2009.
8. Talor, R. H. Funda, J. Eldridge, B. Gomory, S. Gruben, K. LaRose, D. Talamini, M. Kavoussi, L. Anderson. A telerobotic assistant for laparoscopic surgery, IEEE

- Engineering in Medicine and Biology, Vol. 14, pp.279-288, 1995.
9. Ulrich Seibold, Bernhard Kuebler, Gerd Hirzinger. Prototypic force feedback instrument for minimally invasive robotic surgery. *Medical Robotics*, pp.526, 2008.
 10. U. Seibold, G. Hirzinger. A 6-axis force/torque sensor design for haptic feedback in minimally invasive robotic surgery. *MICROtec 2nd VDE World Microtechnologies Congress*, pp.239-244, 2003.
 11. Akhil J Madhani, Niemeyer Gunter, Salisbury Jr. Kenneth J. The Black Falcon: A teleoperated surgical instrument for minimally invasive surgery. *IEEE/RSJ Int. Conference on Intelligent Robots and Systems*, pp.936-944, 1998.
 12. J. Peirs, J. Clijnen, P. Herijgers, D. Reynaerts, J. Van Brussel, B. Cortevvile, S. Boone. Design of an optical force sensor for force feedback during minimally invasive robotic surgery. *EuroSensors XVII*, pp.1063-1066, 2003.
 13. E. U. Schirmbeck, H. Mayer, I. Nagy, A. Knoll, R. Lange, R. Bauernschmitt. Evaluation of force feedback in minimally invasive robotic surgery. *Biomedizinche Technik*, 49(2), pp108-109, 2004.
 14. Istvan Nagy, Hermann Mayer, Alois Knoll. Application of force feedback in robot assisted minimally invasive surgery. *Proceeding of the EuroHaptics Conference*, pp.240-245, 2004.
 15. B. Deml, T. Ortmaier, H. Weiss. Minimally invasive surgery: Empirical comparison of manual and robot assisted force feedback surgery. *Proceedings of the EuroHaptics Conference*, pp.403-406, 2004.

16. T. Ortmaier, B. Deml, B. Kubler, G. Passig, D. Reintsema, U. Seibold. Robot assisted force feedback surgery. *Advances in Telerobotics*, pp.361-379, 2007.
17. A. M. Okamura. Methods for haptic feedback in teleoperated robot assisted surgery. *The Industrial robot*, pp. 499-508, 2004.
18. Seunghwan Kim, Daehie Hong, Jung-Hoon Hwang, Bongseok Kim, S. W. Choi. Development of an integrated torque sensor-motor module for haptic feedback in teleoperated robot-assisted surgery. *Technologies for Practical Robot Applications*, pp.10-15, 2009.
19. G. S. Guthart, J. K. The intuitive telesurgery system: Overview and application. *IEEE International Conference on Robotics and Automation*, Vol. 1, pp.618-621, 2000.
20. Gerhard F. Buess, Marc O. Schurr, Sabine C. Fischer. Robotics and allied technologies in endoscopic surgery. *Archives of Surgery*, Vol. 135, pp.229-234 2000.
21. Ryan E Schoonmaker, Caroline G L Cao. Vibrotactile force feedback system for minimally invasive surgical procedures. *IEEE International Conference on Systems Man and Cybernetics*, pp.2464-2469, 2006.
22. P. Pitakwatchar, S. Warisawa, M. Mitsuishi. Force feedback augmentation method for the minimally invasive surgical system. *Proceedings of the IEEE/RSJ International Conference on Intelligent Robots and Systems*, pp.1564-1569, 2006.
23. P. Pitakwatchara, S. Warisawa, M. Mitsuishi. Analysis of the surgery task for the force

feedback amplification in the minimally invasive surgical system. Proceedings of the International Conference of IEEE Engineering in Medicine and Biology Society, pp.829-832, 2006.

24. M. Tavakoli, R. V. Patel, M. Moallem. A force reflective master-slave system for minimally invasive surgery. Proceeding IEEE/RSJ International Conference on Intelligent Robots and Systems, Vol. 3, pp.3077-3082, 2003.
25. Martin O Culjat, James W Bisley, Chih-Hung King, Christopher Wottawa, Richard E Fan, Erik P Dutson, Warren S Grundfest. Tactile feedback in surgical robotics. Surgical Robotics Systems Applications and Visions, pp.449-468, 2010.
26. M. Kitagawa, A. M. Okamura, B. T. Bethea, V. L. Gott, W. A. Baumgartner. Analysis of suture manipulation forces for teleoperation with force feedback. Medical Image Computing and Computer Assisted Intervention MICCAI, pp.155-162, 2002.
27. Allison M Okamura, Lawton N Verner, Tomonori Yamamoto, James C Gwilliam, Paul G Griffiths. Force feedback and sensory substitution for robot-assisted surgery. Surgical Robotics, pp.419-448, 2011.